Using HERA Data to Determine the Infrared Behaviour of the BFKL Amplitude

with L.N. Lipatov, D.A. Ross and G. Watt
arXiv 1005.0355

Short overview of HERA data - evidence for Pomeron
Discreet Pomeron of BFKL
Correspondence to ADS/CFT Pomeron - talk by M. Djuric

H. Kowalski
11th Workshop on Non-Perturbative QCD
Paris, 7th of June 2011

HERA: the largest e-p collider ever build

Operated between 1992 and 2007

Partons vs Dipoles

Infinite momentum frame: Partons

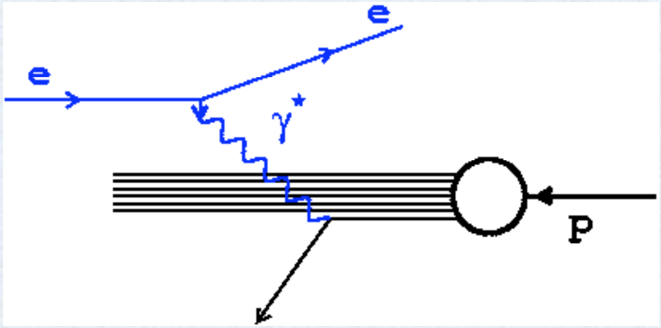

F_2 measures parton density at a scale Q^2

$$F_2 = \Sigma_f \, e_f^2 \, xq(x, Q^2)$$

Proton rest frame: Dipoles - long living quark pair interacts with the gluons of the proton *dipole life time ≈ 1/(m_p x) = 10 - 1000 fm at x = 10^{-2} - 10^{-4}*

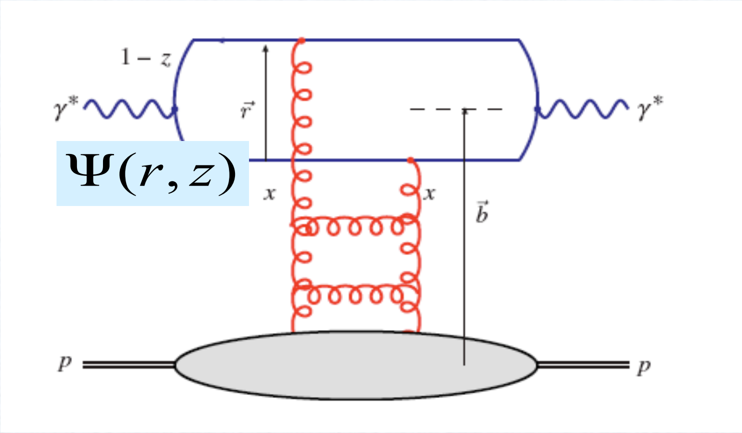

$$\sigma_{tot}^{\gamma^* p} = \int \Psi^* \sigma_{qq} \Psi \; ; \qquad F_2 = \frac{Q^2}{4\pi^2 \alpha_{em}} \sigma_{tot}^{\gamma^* p}$$

for small dipoles, at low-x, dipole picture is equivalent to the QCD parton picture

HERA - F_2 is dominated by the gluon density at low x

- the same gluon density determines the exclusive and inclusive diffractive processes,
  $\gamma p \Rightarrow J/\psi\ p$, $\gamma p \Rightarrow \varphi p$, $\gamma p \Rightarrow \rho p$, $\gamma p \Rightarrow Xp$,

- **universal gluon density ≡ Pomeron ?**

F_2 VM, Diffraction

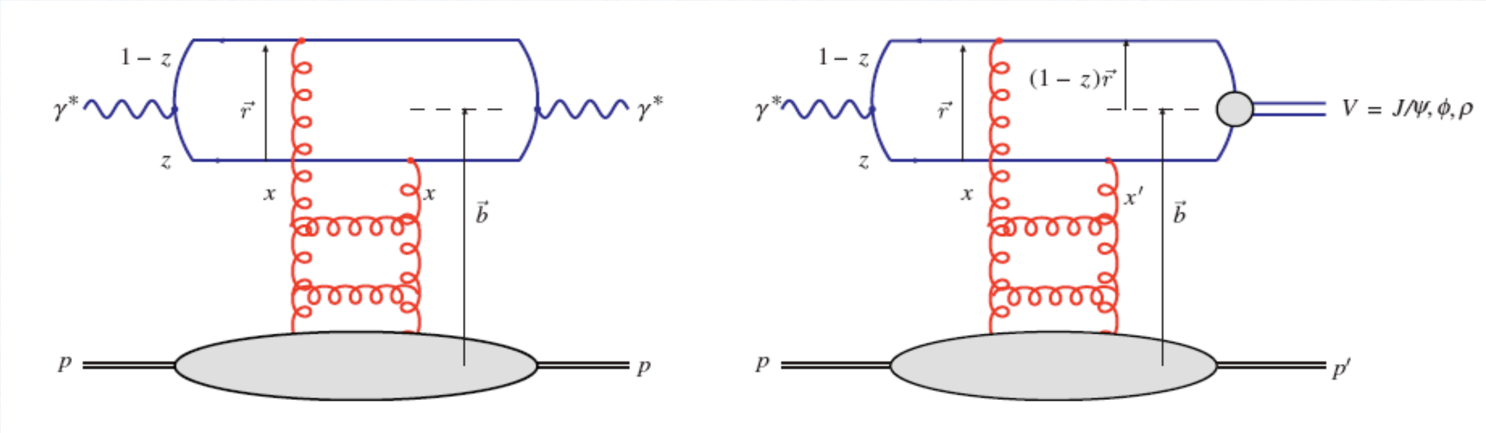

clear hints for saturation, but here we concentrate on the gluon gluon interactions above the saturation region

Diffraction as a shadow of DIS

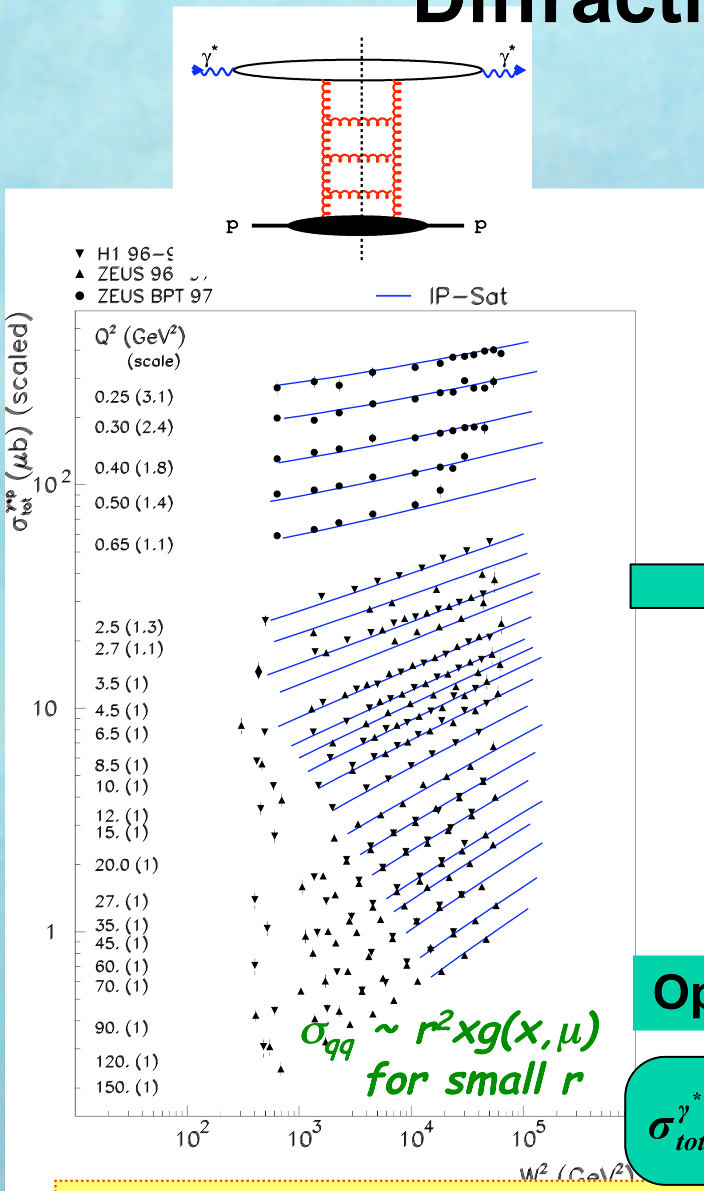

$\sigma_{q\bar{q}} \sim r^2 xg(x,\mu)$

for small r

Optical Theorem

$$\sigma_{tot}^{\gamma^* p} = \frac{1}{W^2} Im A_{el}(W^2)$$

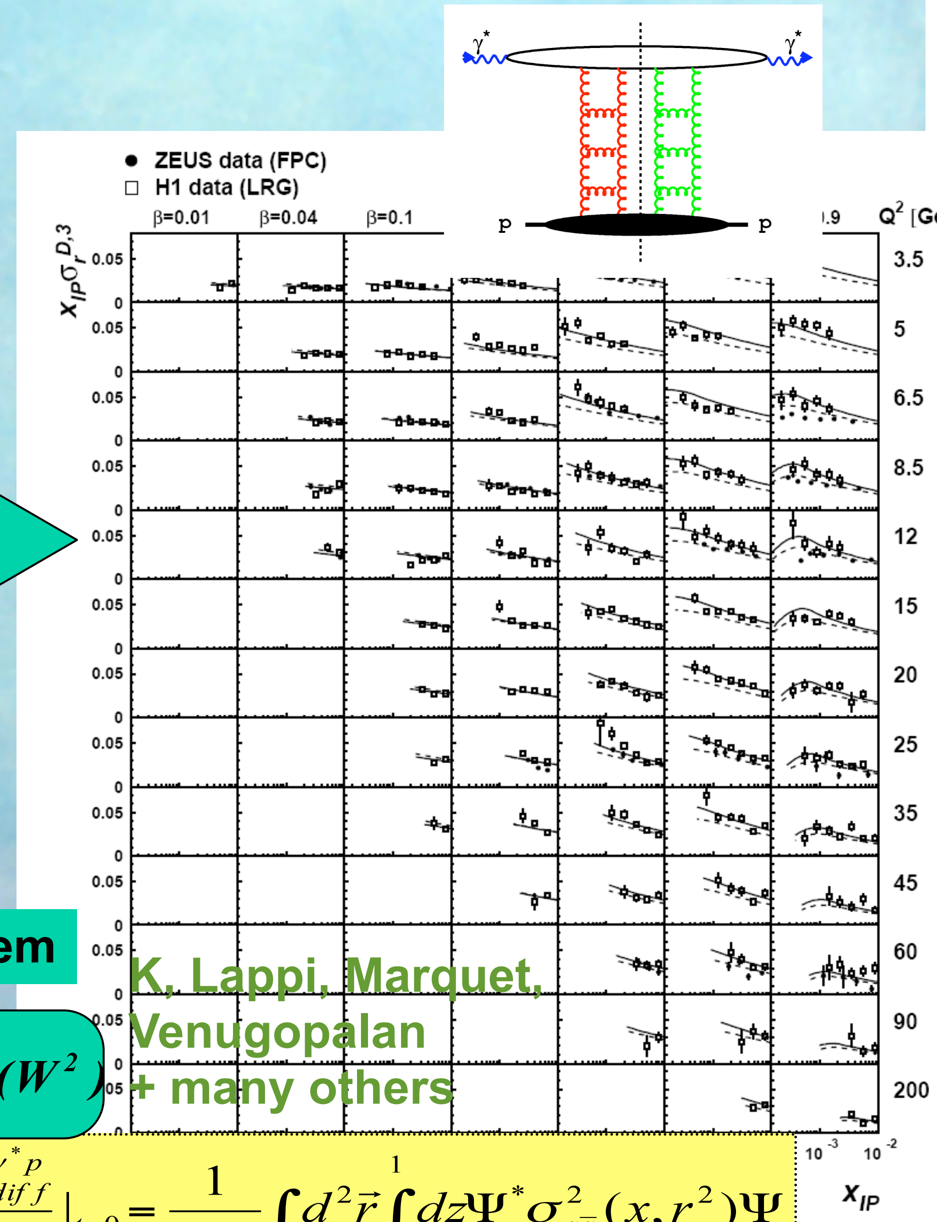

K, Lappi, Marquet, Venugopalan + many others

$$\sigma_{tot}^{\gamma^* p} = \int d^2\hat{\vec{r}} \int_0^1 dz \Psi^* \sigma_{q\bar{q}}(x, r^2) \Psi$$

$$\frac{d\sigma_{diff}^{\gamma^* p}}{dt}\Big|_{t=0} = \frac{1}{16\pi} \int d^2\vec{r} \int_0^1 dz \Psi^* \sigma_{q\bar{q}}^2(x, r^2) \Psi$$

W dependence of exclusive Vector Mesons cross sections

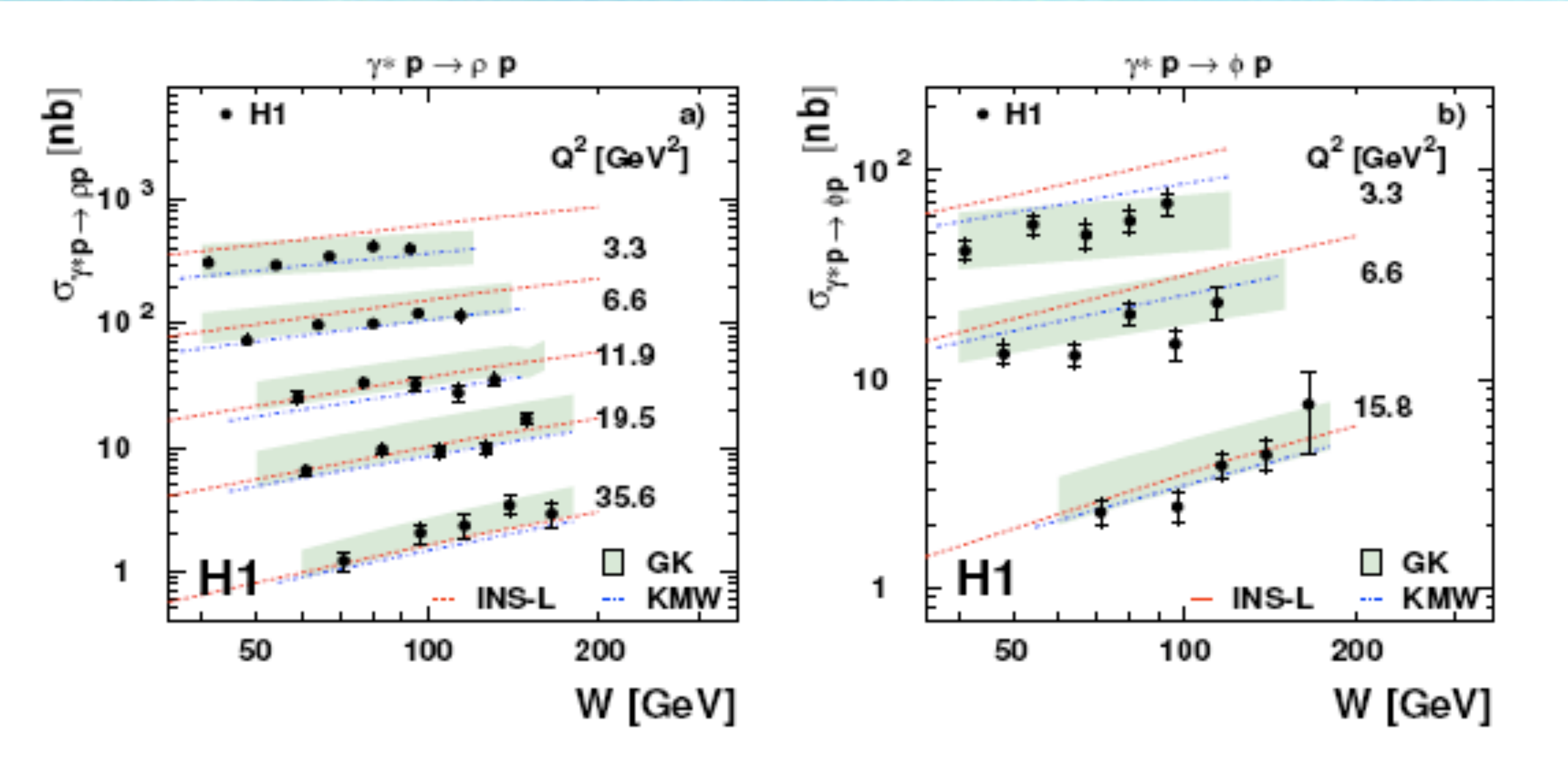

Dipole model with the DGLAP evolution of the gluon density predicts well the rise with W of the ρ and φ VM cross sections

Note: these are absolute predictions obtained from the gluon density determined from F_2

In focus: Exclusive J/psi production

educated guess for VM wf is working very well for J/psi and phi and DVCS

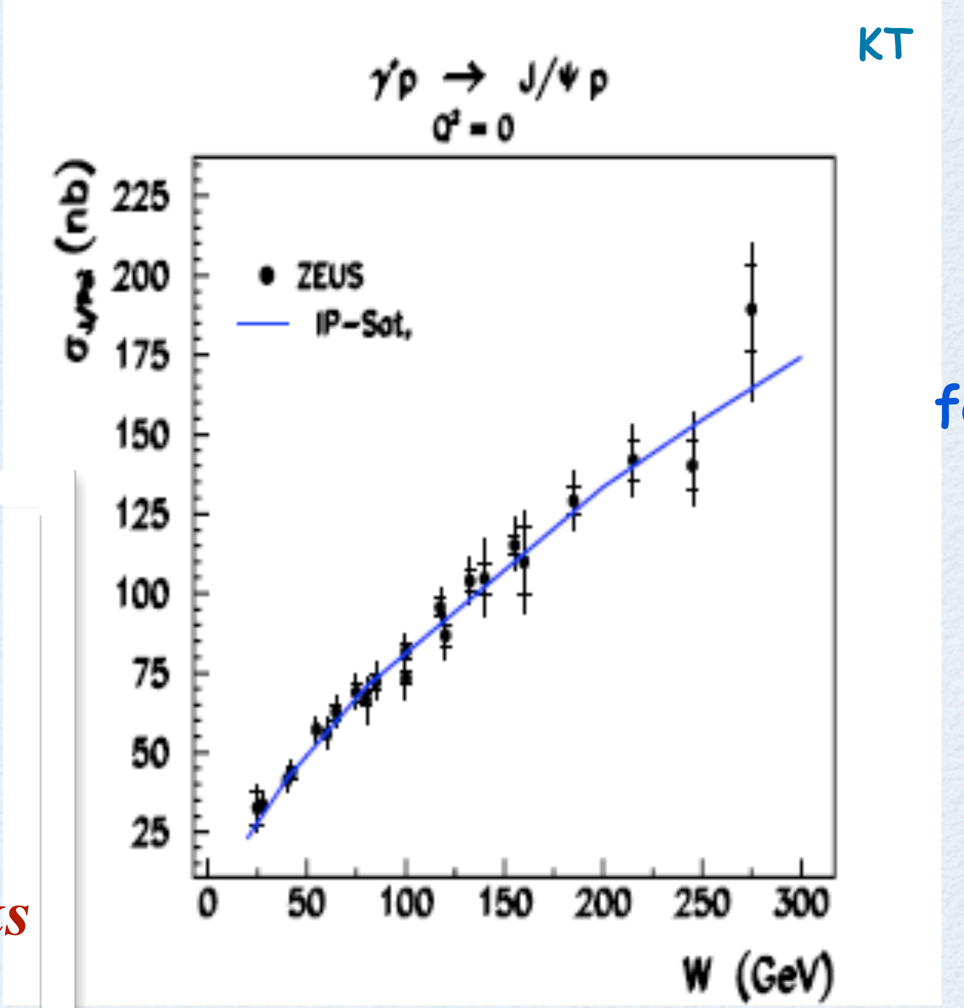

equally good description of Q2 and σ_L/σ_T dependences for J/psi and phi and DVCS

Note:
J/psi x-section grows almost like
$\sigma \propto (x\, g(x,\mu^2))^2$
no valence quarks contribution

➤ **the determination of gluon density with J/psi would be more precise than by F_2 or F_L (MRT) if J/psi would have small systematic errors**

Discovery of HERA: the same, universal gluon density describes different reactions - $\gamma^* p \to X$, $\gamma^* p \to J/\psi\, p$ ...

$\sigma^{\gamma p \to X} \sim W^{2\lambda}$

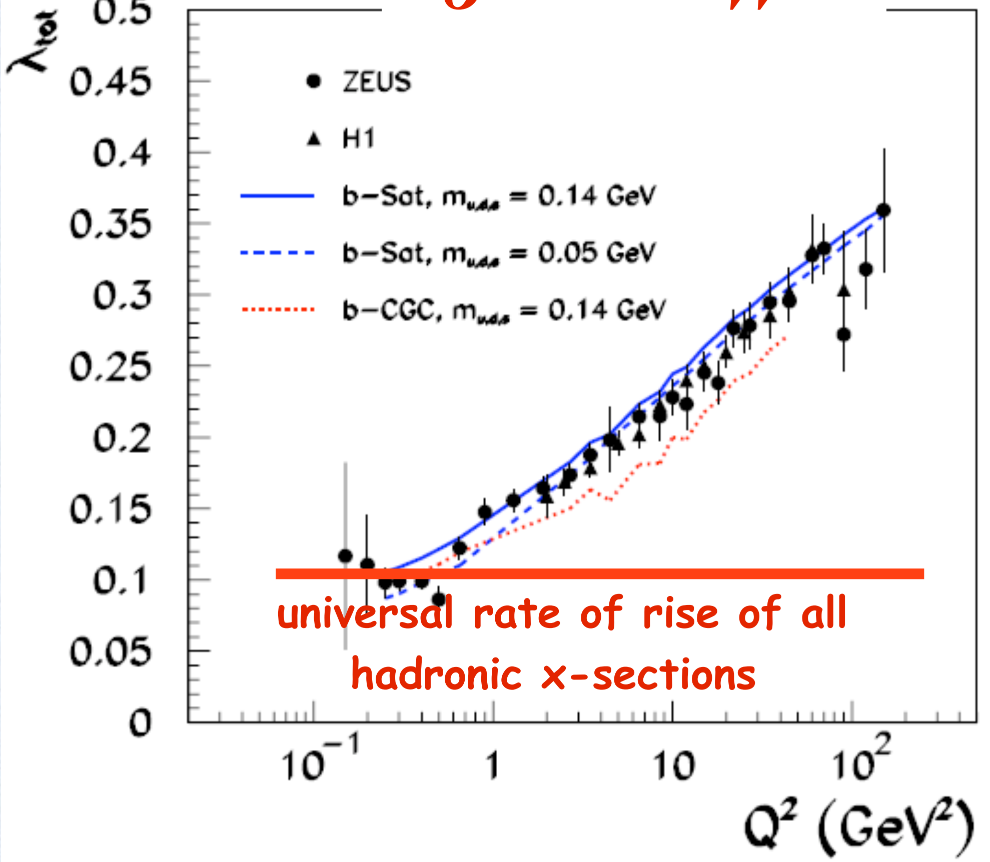

$\sigma^{\gamma p \to J/\psi\, p} \sim W^{\delta}$

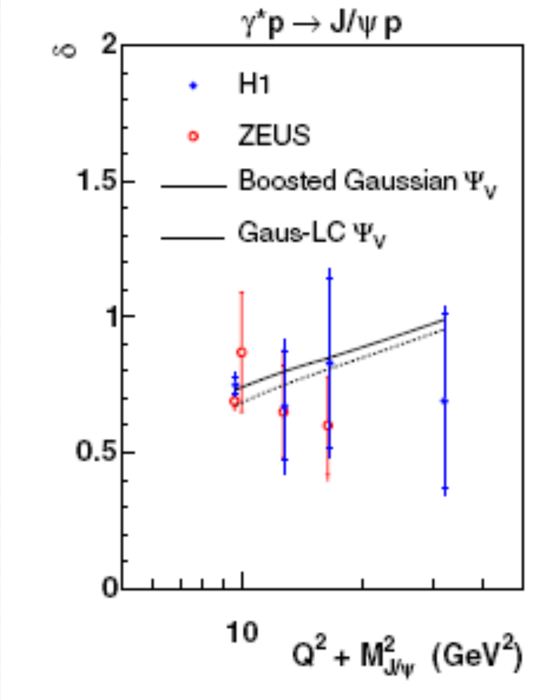

➤ universal, “pomeron like”, QCD object
soft and hard pomeron join together

Extracting Proton Shape using dipoles

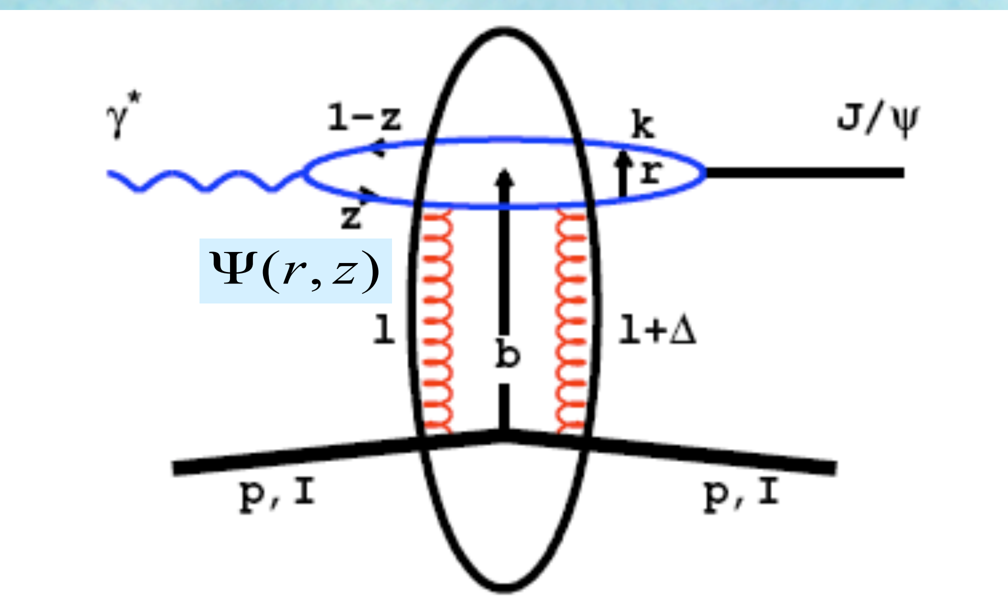

$\Psi(r,z)$

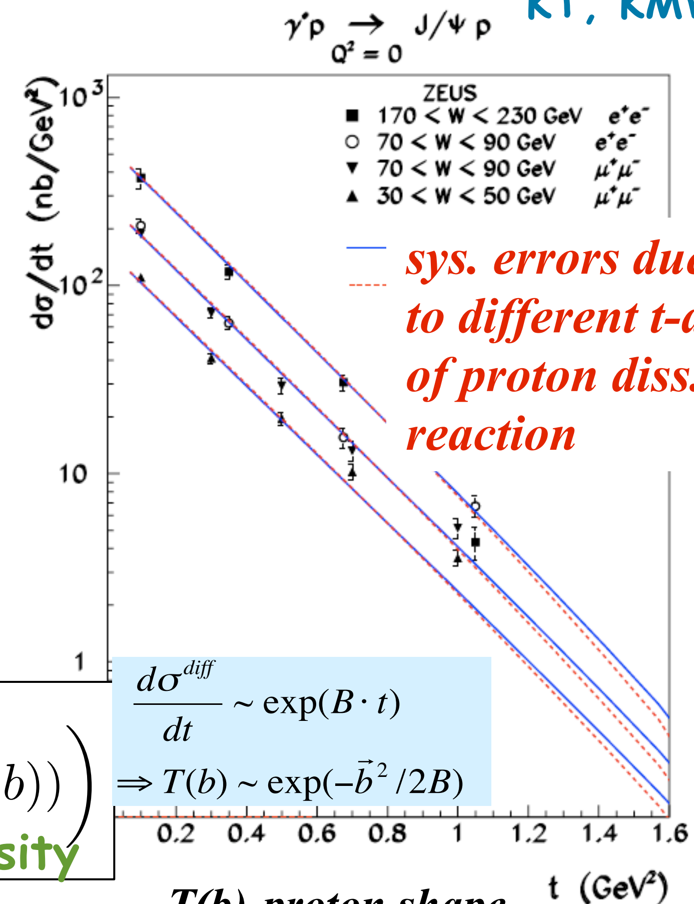

KT, KMW

sys. errors due to different t-dep. of proton diss. reaction

$$\frac{d\sigma^{diff}}{dt} \sim \exp(B\cdot t)$$

$$\Rightarrow T(b) \sim \exp(-\vec{b}^2/2B)$$

T(b)-proton shape

$$\frac{d\sigma_{qq}}{d^2b} = 2\left(1-\exp(-\frac{\pi^2}{2N_C}r^2\,\alpha_s(\mu^2)\,xg(x,\mu^2)\,T(b))\right)$$

for larger gluon density

v.g. description of B for all VM and DVCS with the same wf ansatz
➡ determination of the gluonic proton radius, r_{gg} = 0.6 fm is smaller than the quark radius r_p=0.9 fm

Nuclear gluonic shapes
Coherent and incoherent eA → J/ψA

Dipole projectiles are excellent tools to investigate nuclear matter

measurement precision matches the precision of nuclear physics experiments

AC, HK, PRC 81 025203 (2010)

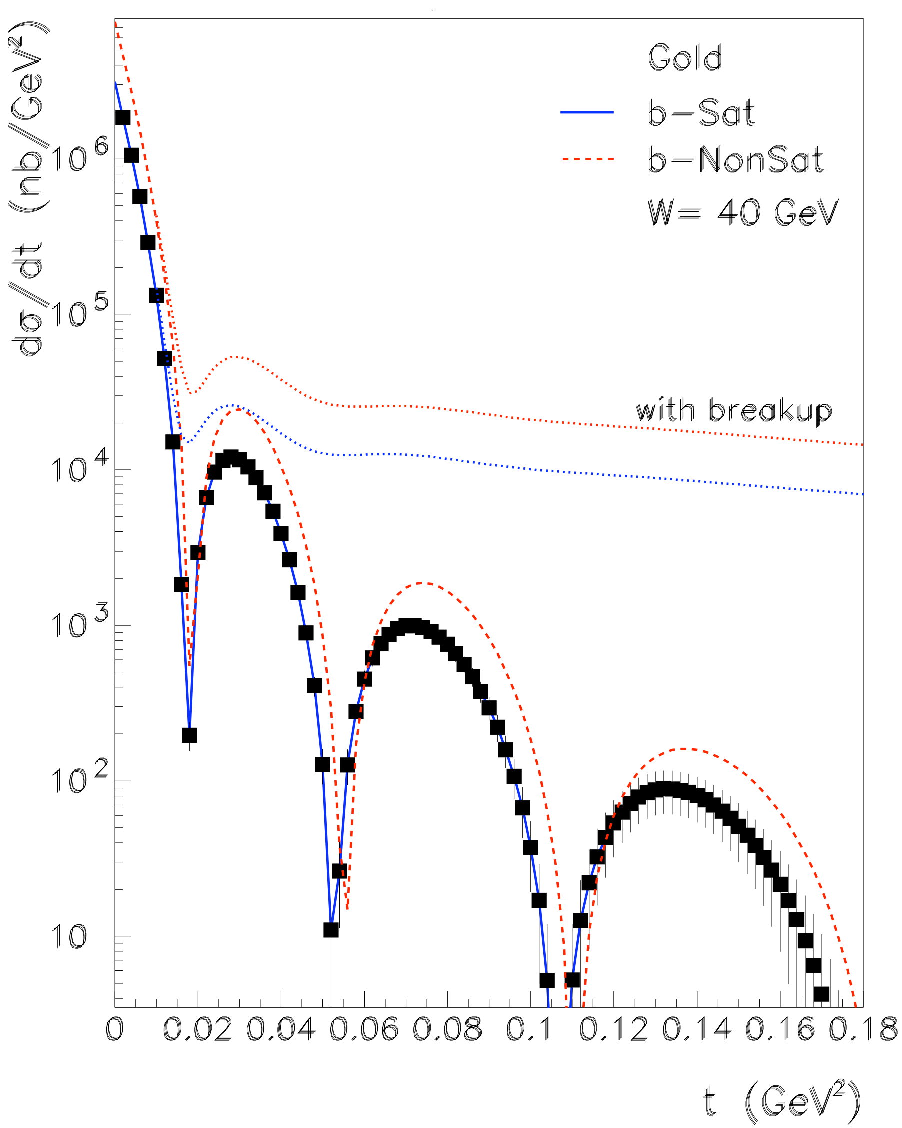

σ_{diff} and σ_{tot} approach saturation in a different way

sensitivity increase due to

$d\sigma_{diff}/dt \propto (x\, g(x,\mu^2))^2$

and

$d\sigma_{diff}/dt|t=0 \sim A^2$

$\sigma_{tot} \sim A$

The dynamics of Gluon Density at low x is determined by **the amplitude for the scattering of a gluon on a gluon**, described by the BFKL equation

$$\frac{\partial}{\partial \ln s}\mathcal{A}(s,\mathbf{k},\mathbf{k}') = \delta(k^2 - k'^2) + \int dq^2 \mathcal{K}(\mathbf{k},\mathbf{q})\mathcal{A}(s,\mathbf{q},\mathbf{k}')$$

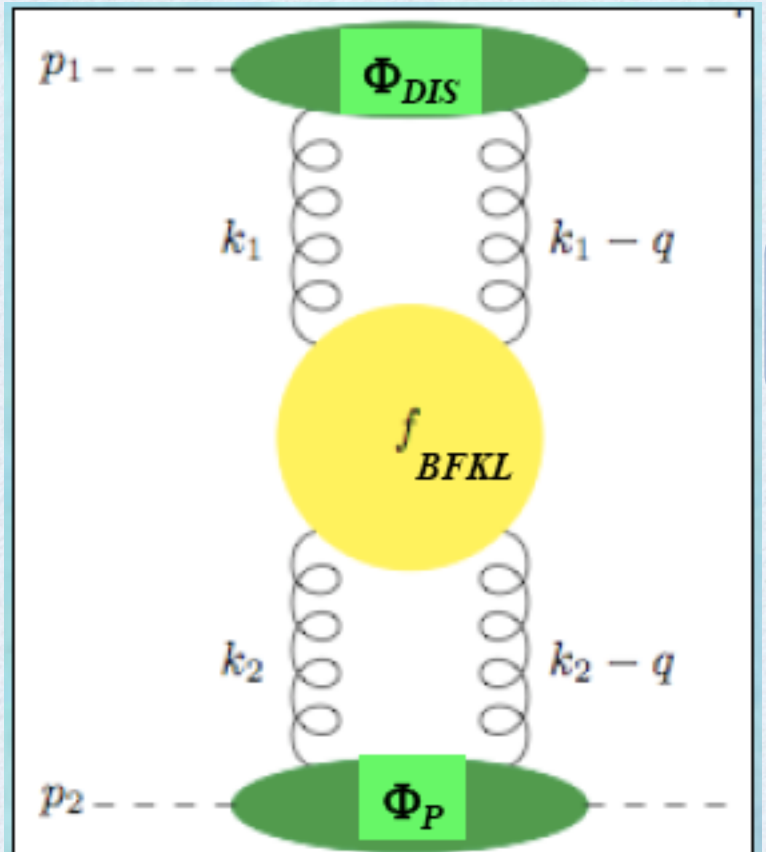

which can be solved in terms of the eigenfunctions of the kernel

$$\int dk'^2 \mathcal{K}(\mathbf{k},\mathbf{k}') f_\omega(\mathbf{k}') = \omega f_\omega(\mathbf{k})$$

in LO, with fixed α_s

$$f_\omega(\mathbf{k}) = \left(k^2\right)^{i\nu - 1/2}$$
$$\omega = \alpha_s \chi_0(\nu)$$

prevailing intuition (based on DGLAP) - gluon are a gas of particles

BFKL leads to a richer structure - basic feature: oscillations

Properties of the BFKL Kernel

Quasi-locality

$$\mathcal{K}(\mathbf{k},\mathbf{k}') = \frac{1}{kk'}\sum_{n=0}^{\infty} c_n \delta^{(n)}\left(\ln(\mathbf{k}^2/\mathbf{k}'^{\,2})\right)$$

$$c_n = \int_0^\infty dk'^{\,2}\mathcal{K}(\mathbf{k},\mathbf{k}')\frac{k}{k'}\frac{1}{n!}\left(\ln(\mathbf{k}^2/\mathbf{k}'^{\,2})\right)^n$$

Similarity to the Schroedinger equation

$$k\int dk'^{\,2}\mathcal{K}(\mathbf{k},\mathbf{k}')f_\omega(\mathbf{k}') = \sum_{n=0}^{\infty} c_n\left(\frac{d}{d\ln(\mathbf{k}^2)}\right)^n \bar{f}_\omega(\mathbf{k}) = \omega\bar{f}_\omega(\mathbf{k})$$

Characteristic function

$$k\int dk'^{\,2}\mathcal{K}(\mathbf{k},\mathbf{k}')f_\omega(\mathbf{k}') = \chi\left(-i\frac{d}{d\ln k^2},\alpha_s(k^2)\right)\bar{f}_\omega(k) = \omega\bar{f}_\omega(k)$$

BFKL amplitude

$$A(s,\mathbf{k_1},\mathbf{k_2}) \sim \int d\nu \left[\frac{\mathbf{k_1^2}}{\mathbf{k_2^2}}\right]^{i\nu} s^{\bar{\alpha}_s \chi(\nu)}$$

$$\bar{\alpha}_s = C_A \frac{\alpha_s}{\pi}$$

Diffusion approximation

$$\chi(\nu) = 4\ln(2) - 7\zeta(3)\nu^2 + \ldots$$

$$\mathcal{A}(s,t,\mathbf{k_1},\mathbf{k_2}) \sim \int d\nu\, s^{1+\overline{\alpha_s}\left(4\ln(2)-7\zeta(3)\nu^2+\cdots\right)} e^{i\nu(ln(\mathbf{k_2})-ln(\mathbf{k_1}))}$$

not a good approximation for BFKL because ν ~ 0.6, sl

exact result in ADS/CFT
talk of M. Djuric

$$\chi = -\frac{(4+\nu^2)}{R^2}$$

BFKL eq., with fixed α_s, predicts $F_2 \sim (1/x)^{\omega}$ with $\omega \sim$ constant with Q^2, $\omega \sim 0.5$ in LO and $\omega \sim 0.3$ in NLO

Therefore, the prevailing opinion was that the BFKL analysis is not applicable to HERA data.

The rate of rise λ

$F_2 \sim (1/x)^{\lambda}$

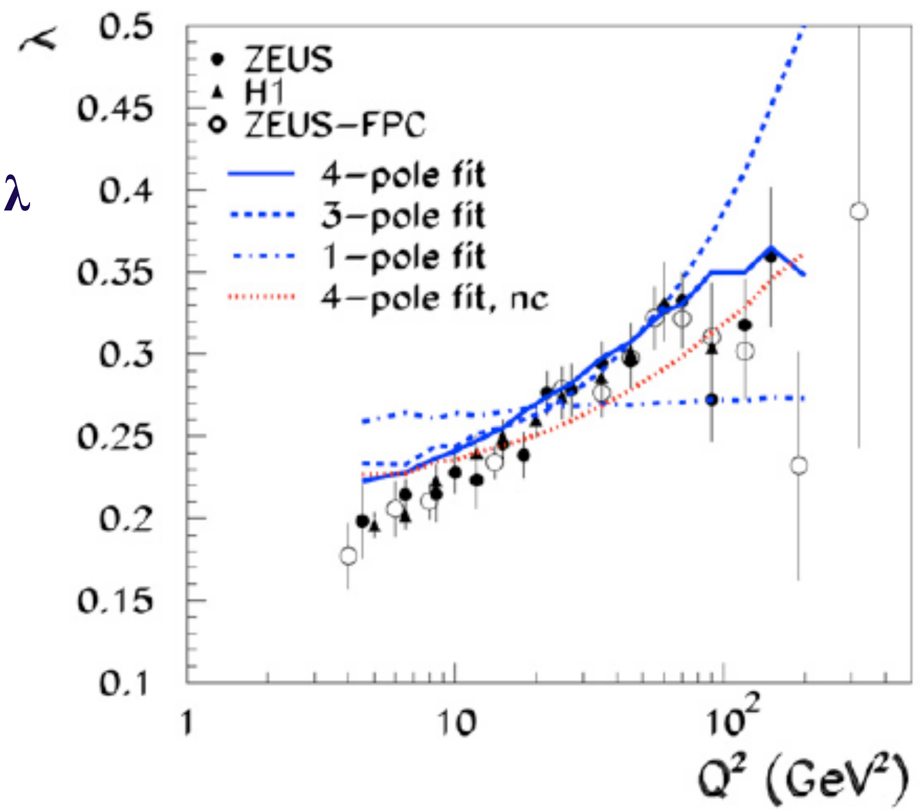

First hints that in BFKL λ can be substantially varying with Q^2 was given in PL 668 (2008) 51 by EKR

Lipatov 86 & EKR 2008: BFKL solutions with the running α_s are substantially different from solutions with the fixed α_s.

in NLO, with running α_s, BFKL frequency ν becomes k-dependent, $\nu(k)$

$$\alpha_s(k^2)\chi_0(\nu(\mathbf{k})) + \alpha_s^2(k^2)\chi_1(\nu(\mathbf{k})) \;=\; \omega$$

ν has to become a function of k because ω cannot depend on k

GS resummation applied

evaluation in diffusion ($\nu \approx 0$) or semiclassical approximation ($\nu > 0$)

For sufficiently large k, there is no longer a real solution for ν.

The transition from real to imaginary $\nu(k)$ singles out a special value of

$$k = k_{crit}, \text{ with } \nu(k_{crit}) = 0.$$

The solutions below and above this critical momentum k_{crit} have to match. This fixes the phase of ef's.

$$k\int dk'^{\,2}\mathcal{K}(\mathbf{k},\mathbf{k}')f_\omega(\mathbf{k}') \;=\; \chi\left(-i\frac{d}{d\ln k^2},\alpha_s(k^2)\right)\bar{f}_\omega(k) \;=\; \omega\bar{f}_\omega(k)$$

semiclassical approximation

$$\left(\frac{d}{d\ln(k)}\right)^r\bar{f}_\omega(k) \;\approx\; \bar{f}_\omega(k)\left(\frac{d\ln\bar{f}_\omega(k)}{d\ln k}\right)^r$$

$$\chi\left(-i\frac{d\ln\bar{f}_\omega(k)}{d\ln k^2},\alpha_s(k^2)\right) \;=\; \omega$$

$$\frac{d\bar{f}_\omega(k)}{d\ln(k^2)} \;=\; i\nu_\omega(\alpha_s(k^2))\bar{f}_\omega(k)$$

DGLAP

Near $k=k_{crit}$, the BFKL eq. becomes the Airy eq. which is solved by the Airy eigenfunctions

$$k\, f_\omega(k) = \bar{f}_\omega(k) = \mathrm{Ai}\left(-(\frac{3}{2}\phi_\omega(k))^{\frac{2}{3}}\right)$$

with

$$\phi_\omega(k) = 2\int_k^{k_{\mathrm{crit}}} \frac{d\,k'}{k'} |\nu_\omega(k')|$$

for $k<<k_{crit}$ the Airy function has the asymptotic behaviour

$$k\, f_\omega(k) \sim \sin\left(\phi_\omega(k) + \frac{\pi}{4}\right)$$

The two fixed phases at $k=k_{crit}$ and at $k=k_0$ (near Λ_{QCD}) lead to the quantization condition

$$\phi_\omega(k_0) = \left(n - \frac{1}{4}\right)\pi + \eta\,\pi$$

The first eight eigenfunctions determined at η=0

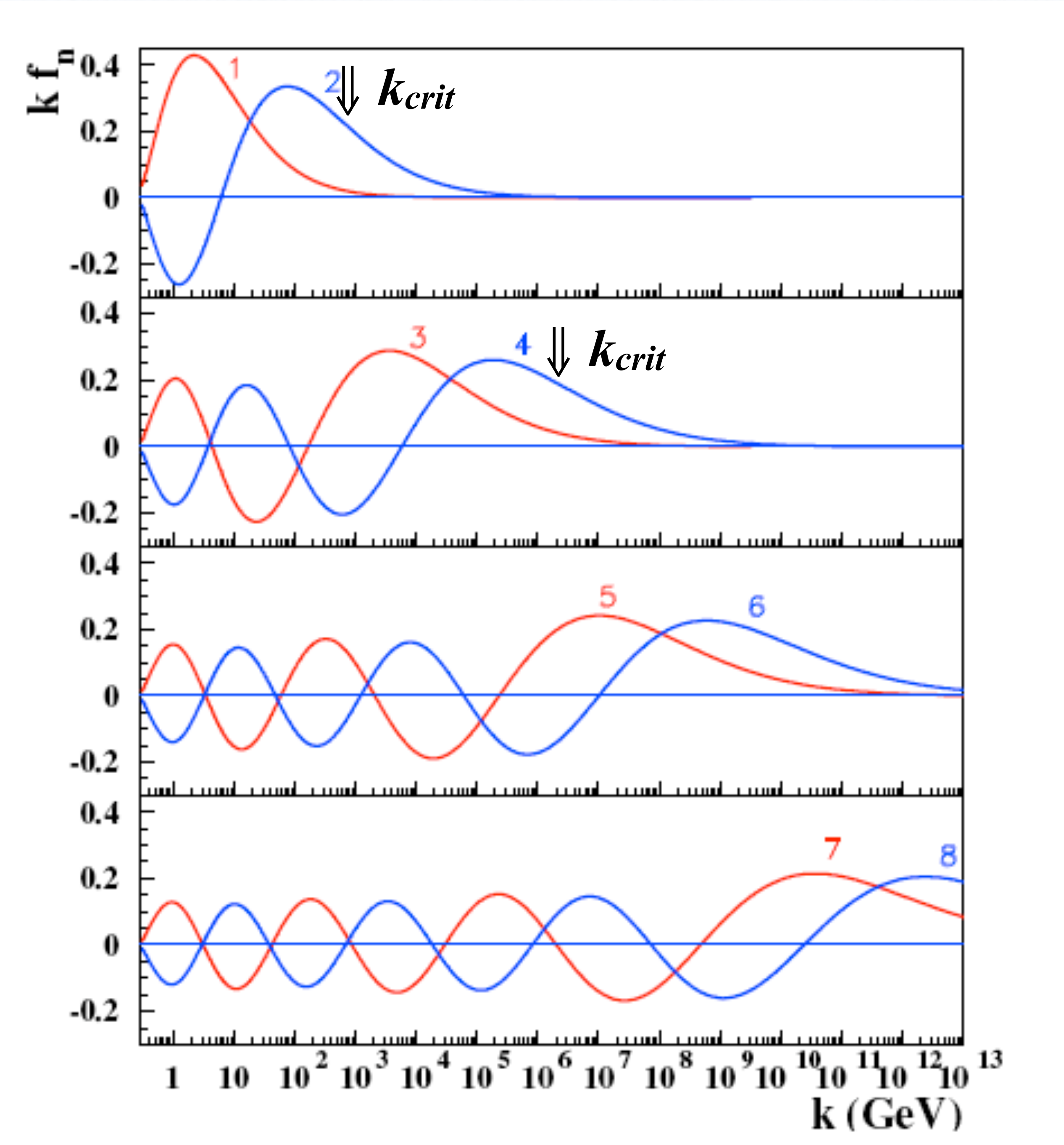

Eigenvalues ω

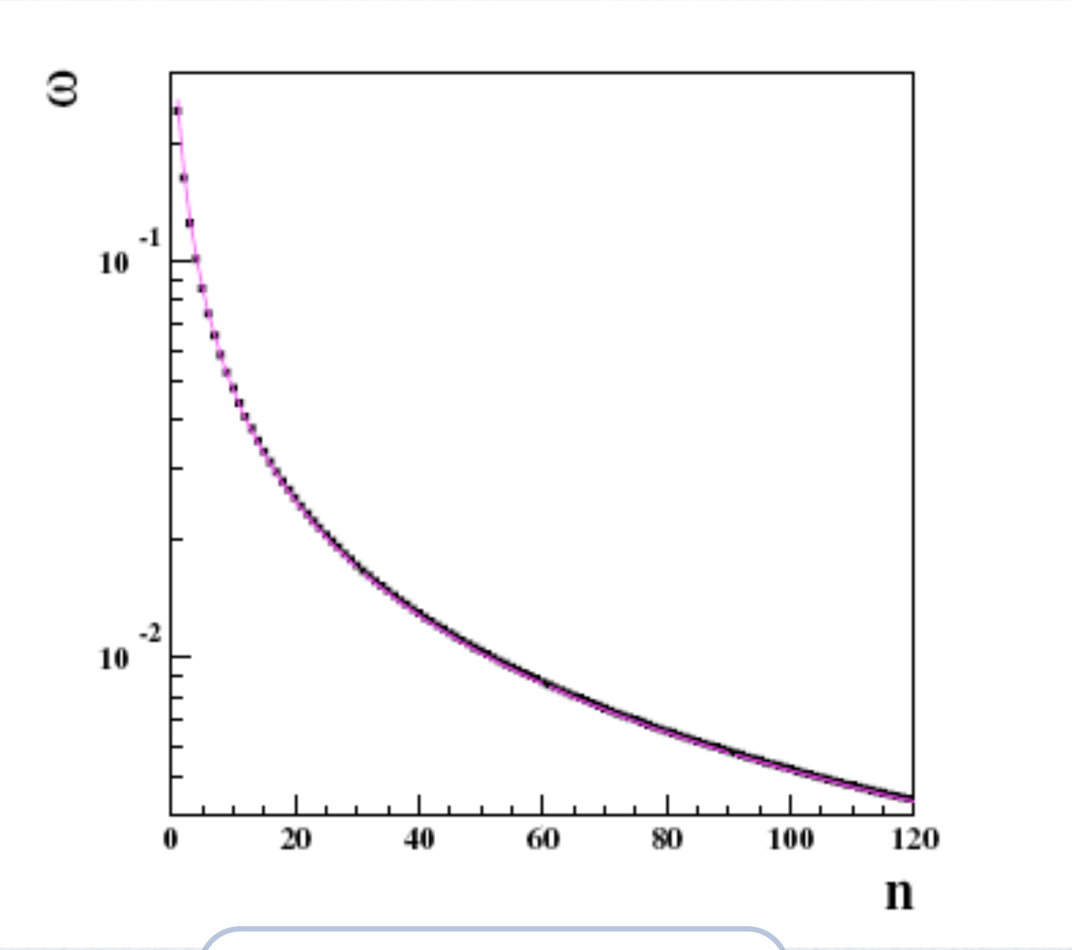

$$\omega_n \approx \frac{0.5}{1 + 0.95\, n}$$

The frequencies *ν(k)*

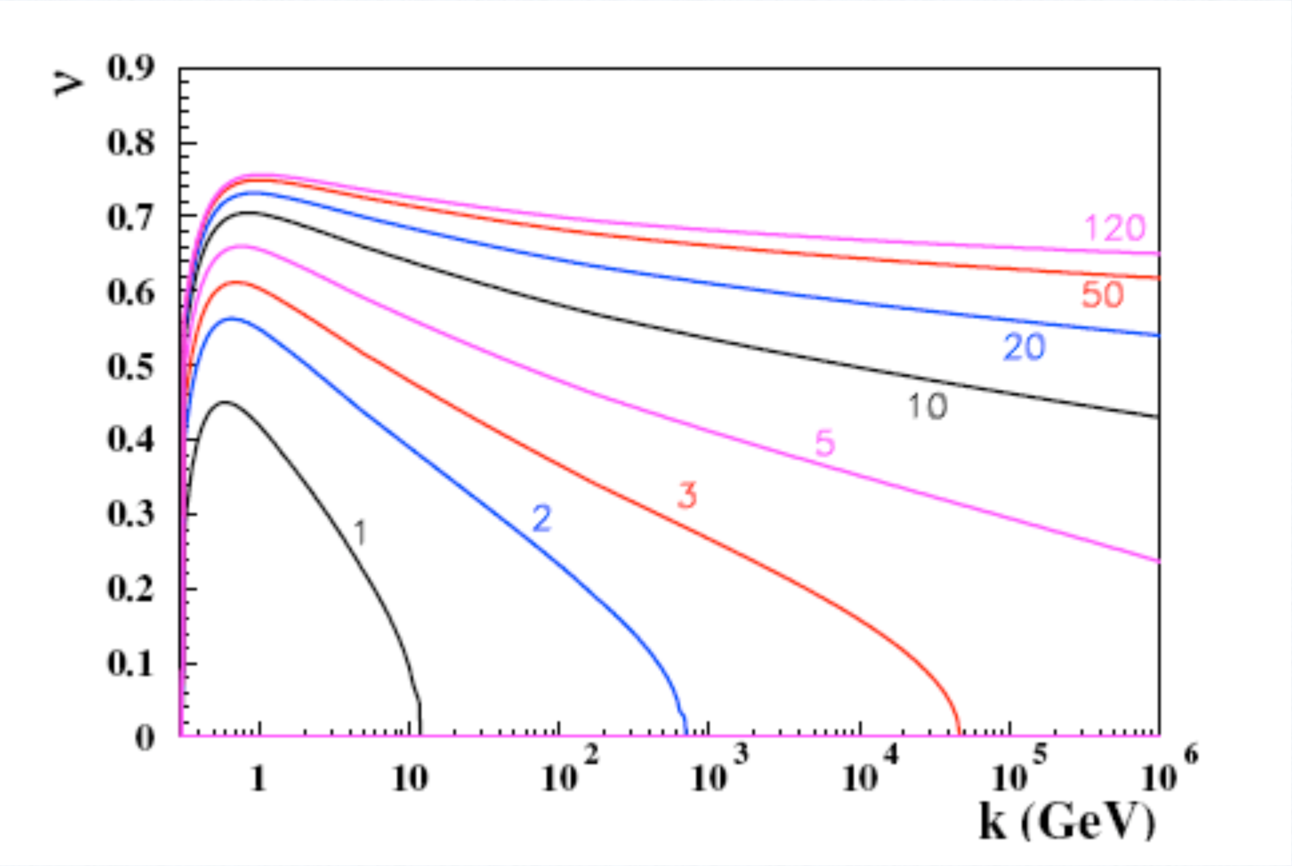

Music analogy:
eigenfunctions are tones with modulated frequencies

Comparison with HERA data

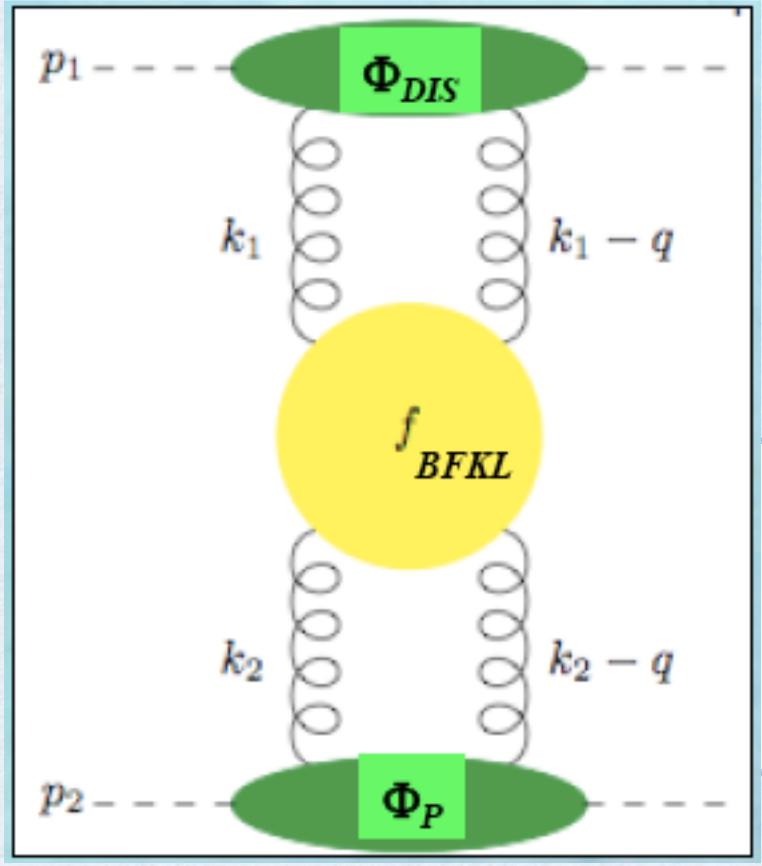

Discreet Pomeron Green function

$$\mathcal{A}(\mathbf{k},\mathbf{k}') = \sum_{m,n} f_m(\mathbf{k}) \mathcal{N}^{-1}_{mn} f_n(\mathbf{k}') \left(\frac{s}{kk'}\right)^{\omega_n}.$$

Integrate with the photon and proton impact factors

$$\mathcal{A}^{(U)}_n \equiv \int_x^1 \frac{d\xi}{\xi} \int \frac{dk}{k} \Phi_{\mathrm{DIS}}(Q^2,k,\xi) \left(\frac{\xi k}{x}\right)^{\omega_n} f_n(\mathbf{k})$$

$$\mathcal{A}^{(D)}_m \equiv \int \frac{dk'}{k'} \Phi_p(k') \left(\frac{1}{k'}\right)^{\omega_m} f_m(\mathbf{k}').$$

$$F_2(x,Q^2) = \sum_{m,n} \mathcal{A}^{(U)}_n \mathcal{N}^{-1}_{nm} \mathcal{A}^{(D)}_m$$

Proton impact factor

$$\Phi_p(\mathbf{k}) \;=\; A\,k^2 e^{-bk^2}$$

The fit is not sensitive to the particular form of the impact factor.

The support of the proton impact factor is much smaller than the oscillation period of f_n and because the frequencies ν have a limited range

- **many eigenfunctions have to contribute and η has to be a function of n**

$$\eta \;= \eta_0 \left(\frac{n-1}{n_{\max}-1}\right)^{\kappa}$$

The qualities of fits for various numbers of eigenfunctions

(a) Fits with cuts of $Q^2 > 4$ GeV^2 and $x < 0.01$

$n_{\max}$	$\chi^2/N_{\rm df}(x<0.01)$	$\chi^2/N_{\rm dat}(x<0.001)$	κ	A	b
1	$9792/125 = 78.3$	$2123/43 = 49.4$	–	156	30.0
5	$349.8/125 = 2.80$	$88.8/43 = 2.07$	3.78	$3.1 \cdot 10^6$	78.0
20	$286.5/125 = 2.29$	$83.3/43 = 1.94$	0.96	632	15.8
40	$193.3/125 = 1.55$	$54.9/43 = 1.28$	0.84	2315	23.2
60	$163.3/125 = 1.31$	$44.8/43 = 1.04$	0.78	3647	25.6
80	$156.5/125 = 1.25$	$43.5/43 = 1.01$	0.73	3081	24.4
100	$149.1/125 = 1.19$	$41.3/43 = 0.96$	0.69	2414	22.8
120	$143.7/125 = 1.15$	$39.2/43 = 0.91$	0.66	2041	21.8

➤ new data are crucial for finding the right solution

the differences in the fit qualities would be negligible if the errors where more than 2-times larger

The final fit performed with 120 ef's and 30 overlaps and 5 flavours

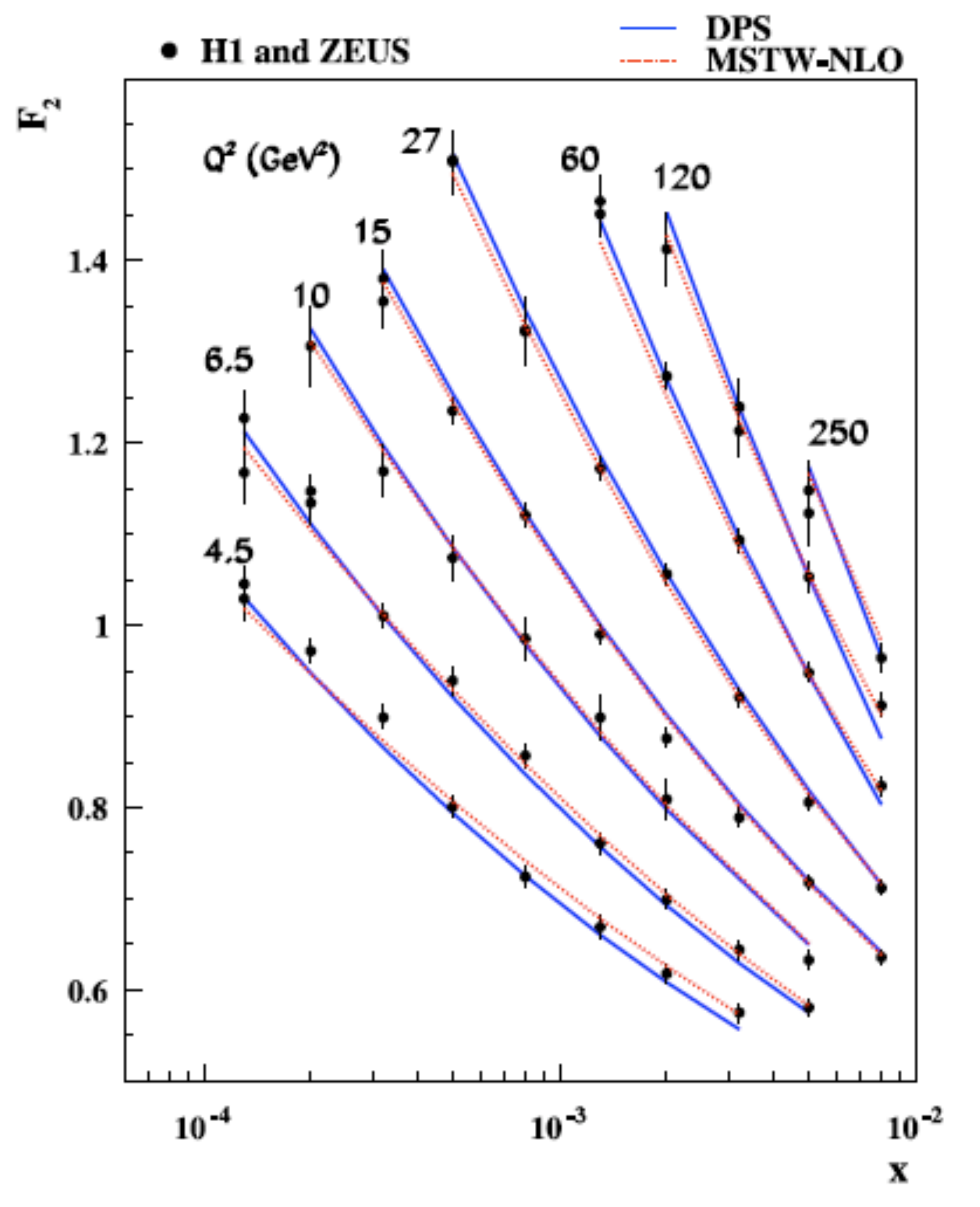

χ^2/N_{df}	κ	A	b
154.7 / 125	0.65	1660	20.6

The rate of rise λ

$F_2 \sim (1/x)^\lambda$

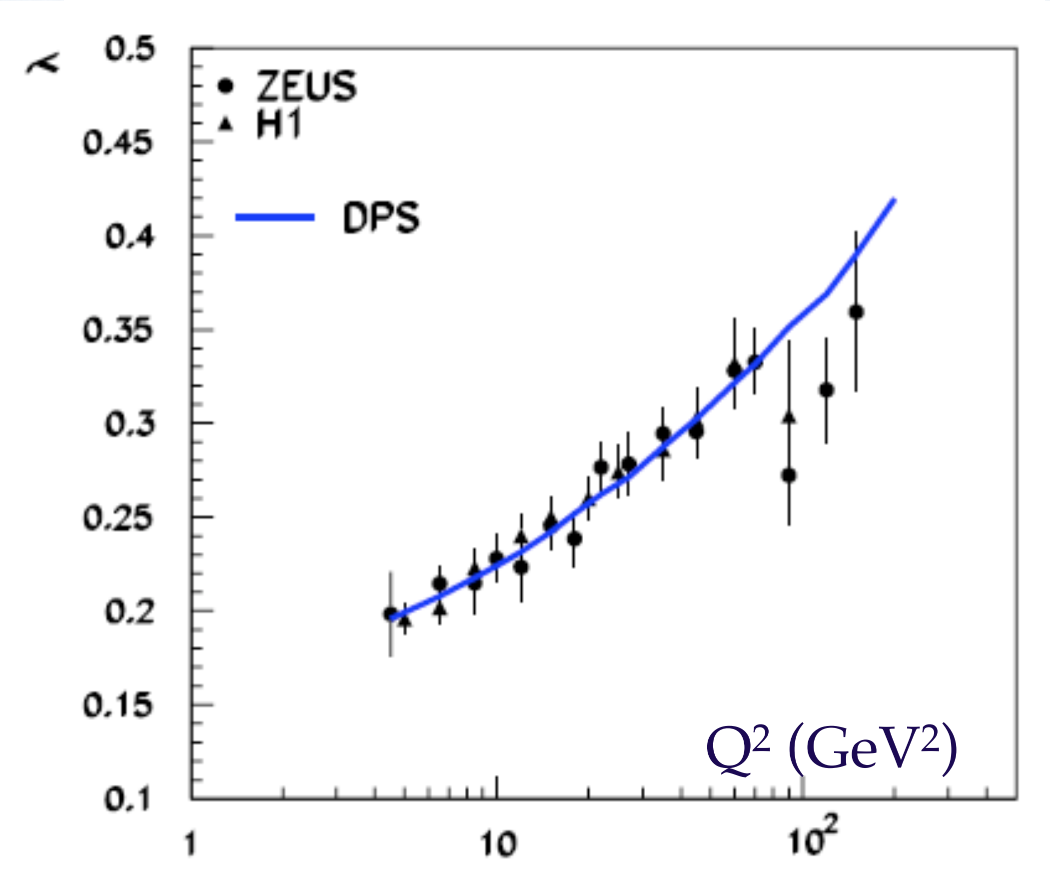

The first successful pure BFKL description of the λ plot.

For many years it was claimed that BFKL analysis was not applicable to HERA data because of the observed substantial variation of λ with Q^2

Pomeron Regge trajectories in ADS

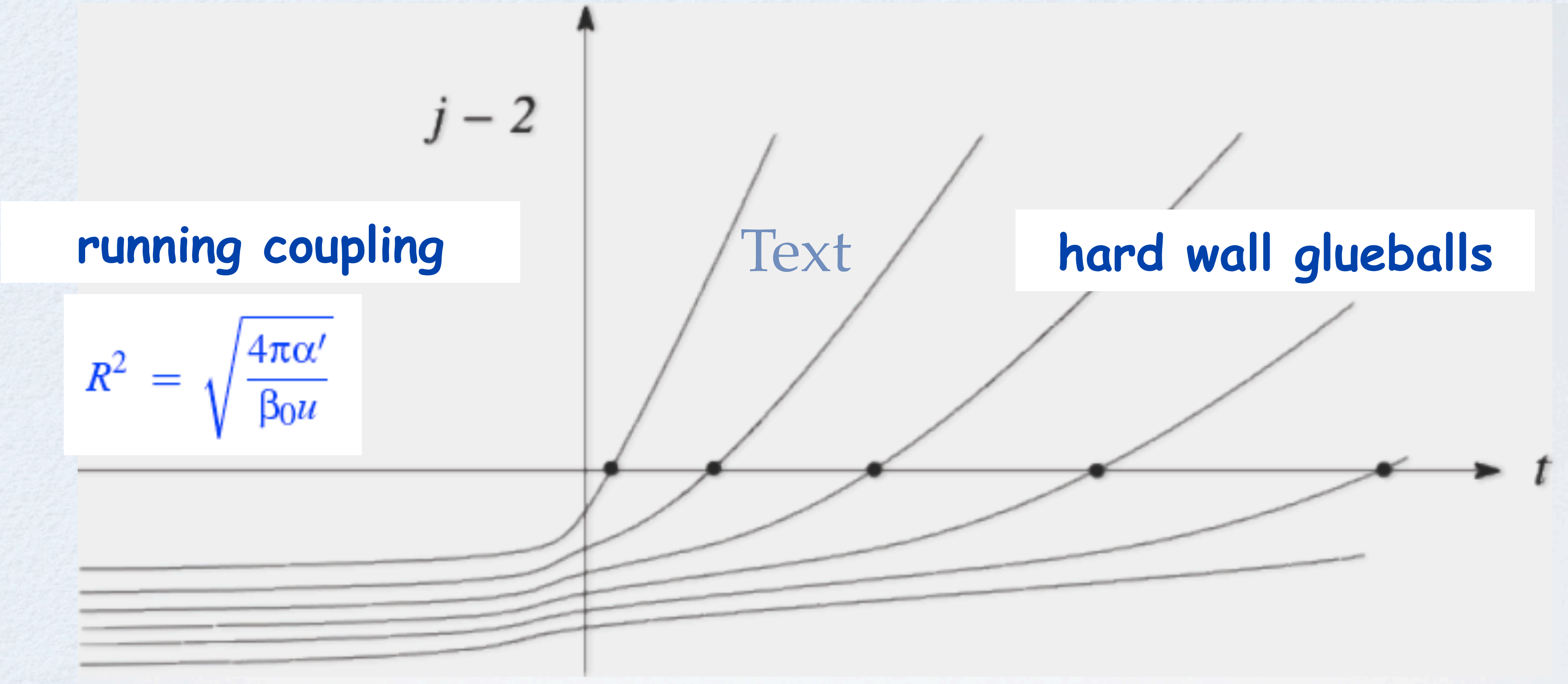

String-Gauge Dual Description of Deep Inelastic Scattering at Small-x

arXiv: 1007.2259v2, Sept 2010

Richard C. Brower,* Marko Djurić,† Ina Sarčević‡§ and Chung-I Tan¶

diffusion term　　reflected term

$$F_2(x,Q^2) = \frac{g_0^2\rho^{3/2}}{32\pi^{5/2}} \int dz dz' P_{13}(z,Q^2) P_{24}(z')(zz'Q^2)\, e^{(1-\rho)\tau} \left(\frac{e^{-\frac{\log^2 z/z'}{\rho\tau}}}{\tau^{1/2}} + \mathcal{F}(z,z',\tau) \frac{e^{-\frac{\log^2 zz'/z_0^2}{\rho\tau}}}{\tau^{1/2}} \right)$$

$$P_{13}(z) \approx C\delta(z-1/Q). \qquad P_{24}(z') \approx \delta(z'-1/Q').$$

$$e^{(1-\rho)\tau} \sim (1/x)^{1-\rho}$$

$$\mathcal{F}(z,z',\tau) = 1 - 2\sqrt{\rho\pi\tau}\, e^{\eta^2} erfc(\eta), \qquad \eta = \frac{-\log\frac{zz'}{z_0^2} + \rho\tau}{\sqrt{\rho\tau}}.$$

reflected term (model dependent) corresponds to the phase condition in KLRW

fitted variables, g_0, ρ, z_0, Q'

in KLRW, ρ is predicted

Discrete BFKL-Pomeron

Summary of properties:

Consists of many eigenfunctions:
the contribution of large n ef's is only weakly suppressed,
enhancement by $(1/x)^{\omega}$ is not very large because
$\omega_1 \approx 0.25, \quad \omega_5 \approx 0.1, \quad \omega_{10} \approx 0.05$
suppression of large n contribution only by the normalization condition $\sim 1/\sqrt{n}$

The shape and normalization of the eigenfunctions is determined by the perturbative QCD:

The phase condition at k_0 is of the non-perturbative origin - confinement property

DP is a transition object from small to large or vice versa

The first eight eigenfunctions determined at $\eta=0$

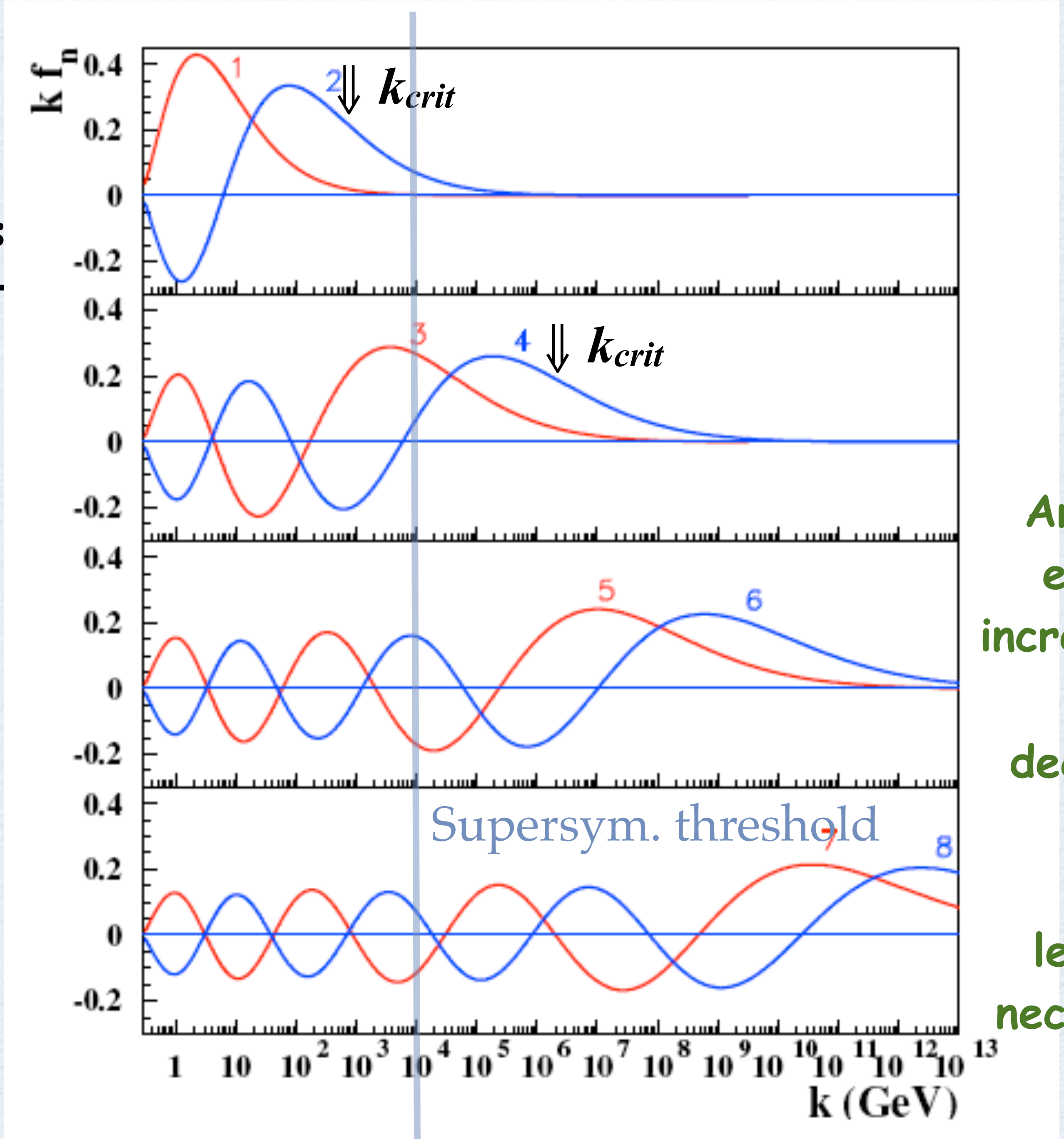

Are BSM effects increasing ν ? and decreasing k_{crit} ?

less ef's necessary ?

Transition to the saturation and confinement regions

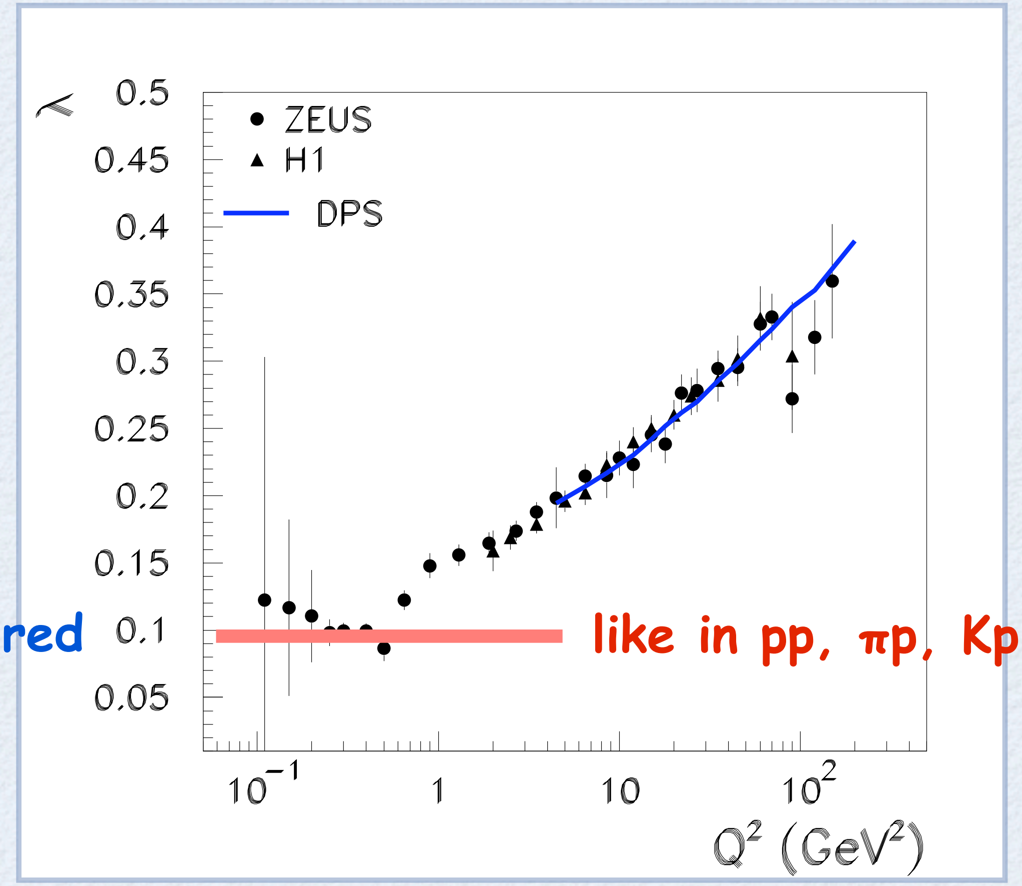

precision data
at low Q^2 required

like in pp, πp, Kp scattering

evaluate triple pomeron vertex with DPS, at $t \neq 0$, apply it in the saturation region, i.e at low Q^2 , and to elastic pp scattering

High energy behaviour of pp, πp, Kp and γp shows universal properties ☞ get insight into confinement?

Summary and Outlook

Since the beginning of particle physics, high energy behavior of scattering amplitudes was expected to give basic insight into the nature of strong forces. At HERA, for the first time, this behavior can be related to properties of the QCD-Pomeron.

Two different basic approaches: the Discrete-BFKL-Pomeron and ADS-closed-string-Pomeron are describing HERA F_2 data very well.

Will striking similarities between the two approaches give insight into the connection between QCD and Gravitation? Into the confinement problem?

Precise measurement at future ep and eA could provide crucial data:

1) exclusive diffractive processes ⇒ measurements of $\alpha(t)$ - EIC

2) F_2 and exclusive diffraction at highest possible energies - LHeC

Back up slides

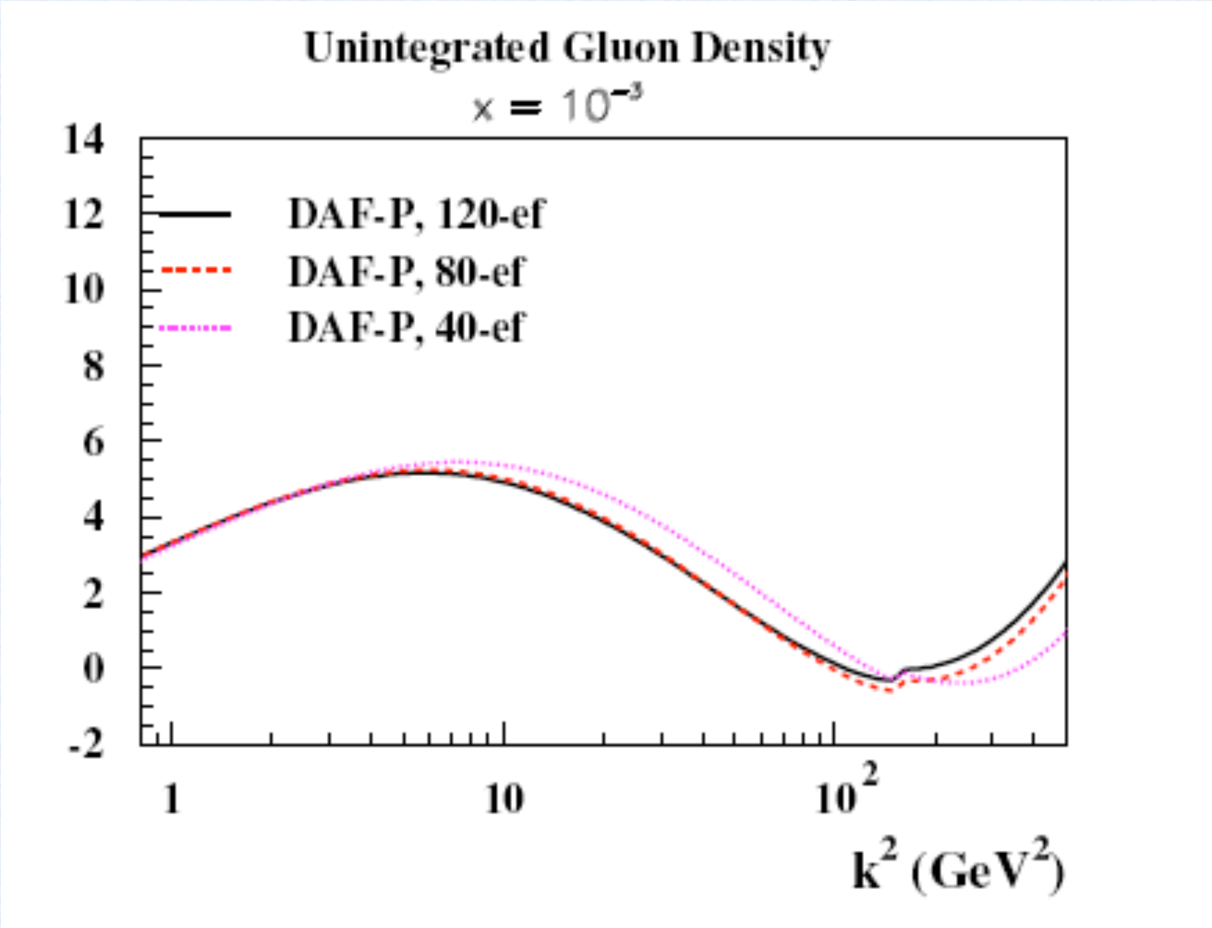

Unintegrated Gluon Density
x = 10⁻³
14
12
10
8
6
4
2
0
-2
DAF-P, 120-ef
DAF-P, 80-ef
DAF-P, 40-ef
1
10
10²
k² (GeV²)

Quasi-locality of the kernel

$$\mathcal{K}(\mathbf{k},\mathbf{k}') = \frac{1}{kk'}\sum_{n=0}^{\infty} c_n \delta^{(n)}\left(\ln(\mathbf{k}^2/\mathbf{k}'^2)\right),$$

and of the Green function

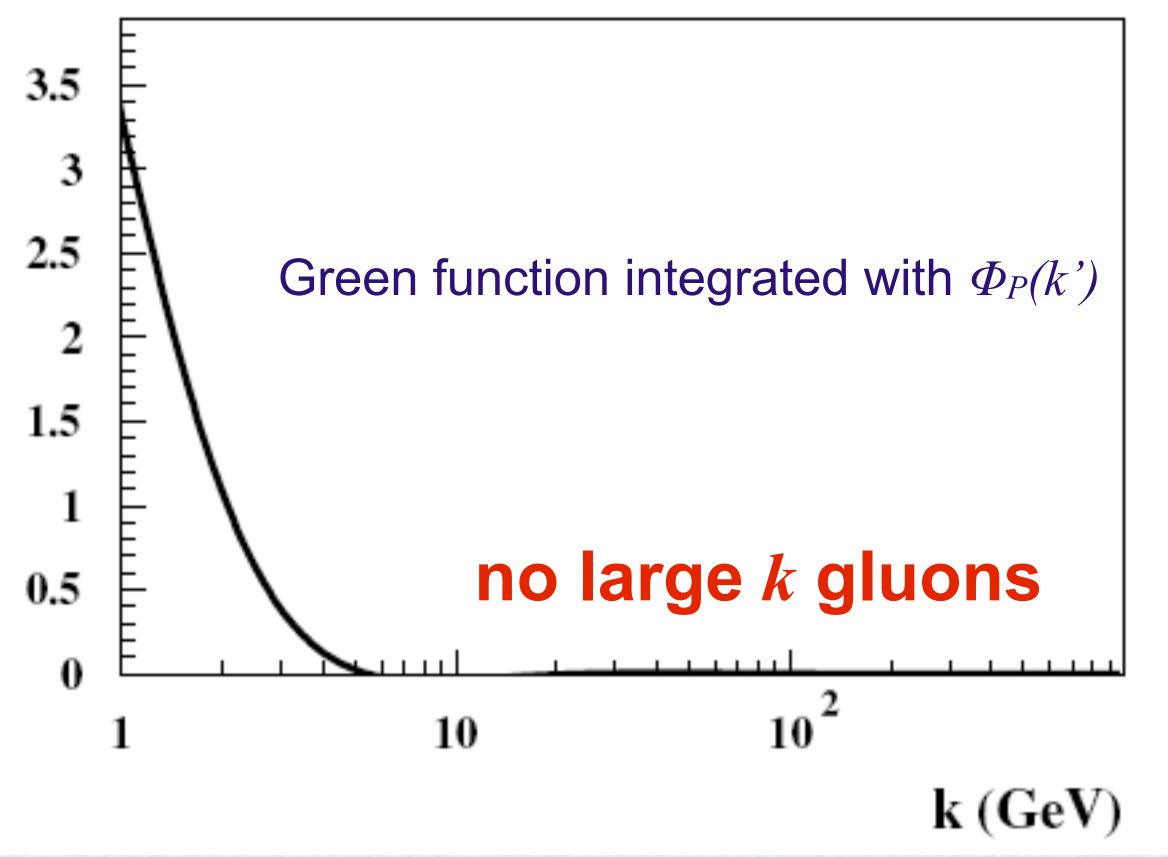

Pomeron - Graviton Correspondence

String theory emerged out of phenomenology of hadron-hadron scattering - Dolan-Horn-Schmid duality

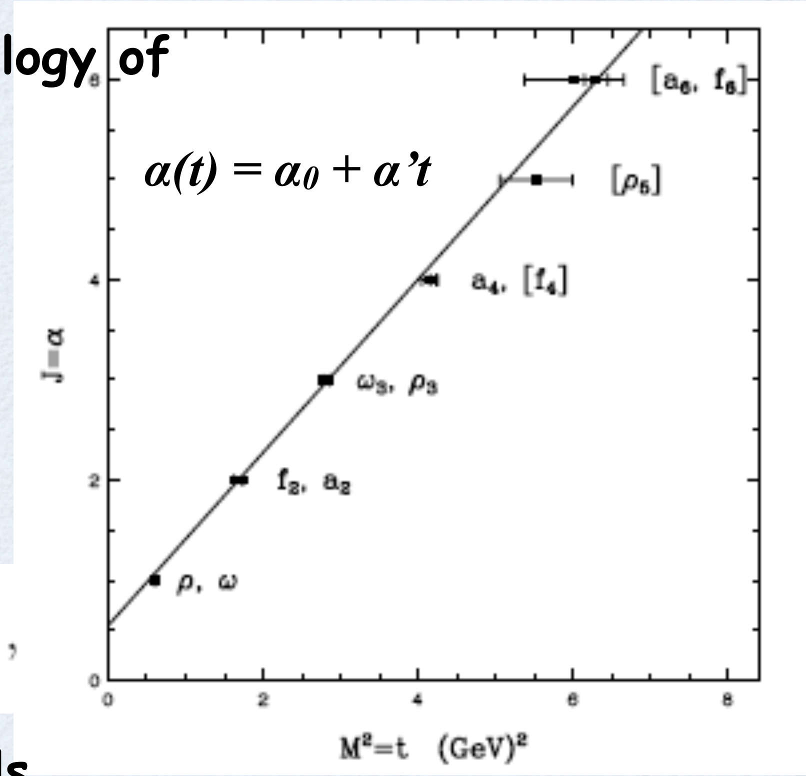

$$\sum_r \frac{g_r^2(t)}{s-(M_r-i\Gamma_r)^2} \simeq \beta(t)(-\alpha' s)^{\alpha(t)}$$

▶ Veneziano amplitude

$$A_{\pi^+\pi^-\to\pi^+\pi^-}(s,t) = g_o^2\,\frac{\Gamma[1-\alpha_\rho(t)]\Gamma[1-\alpha_\rho(s)]}{\Gamma[1-\alpha_\rho(s)-\alpha_\rho(t)]},$$

▶ generalization to dual resonance models, Veneziano amplitude for the pomeron trajectory has a pole for $s=t=0$ *with* $J=2$

▶ starting point for a theory of quantum gravity

Maldacena Conjecture: (N=4 SUSY YM QCD) = (CFT in $ADS_5 \times S^5$)

Pomeron in ADS, Brower, Polchinski, Strassler, Tan, 2006

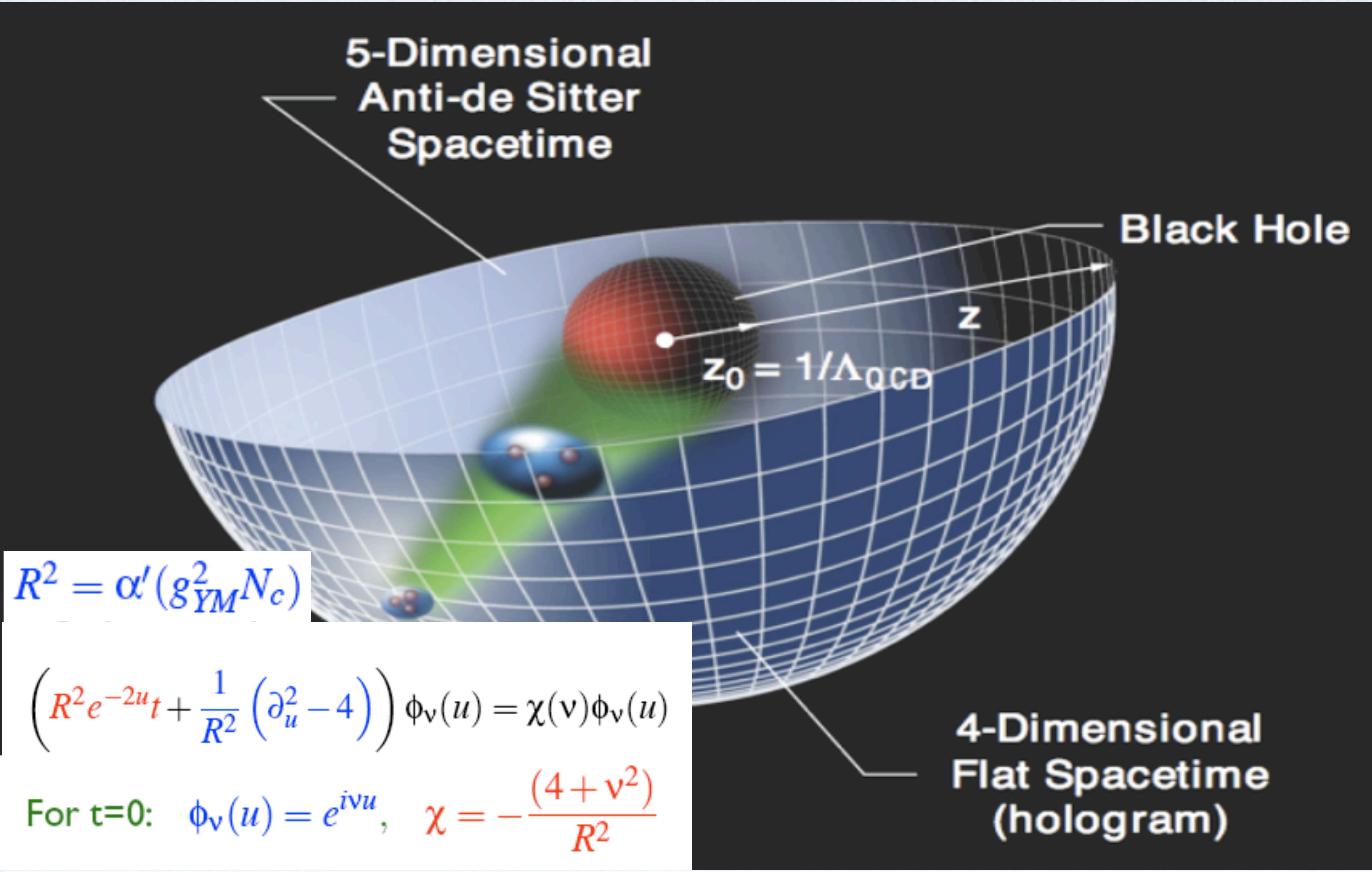

$$R^2 = \alpha'(g_{YM}^2 N_c)$$

$$\left(R^2 e^{-2u} t + \frac{1}{R^2}\left(\partial_u^2 - 4\right)\right)\phi_\nu(u) = \chi(\nu)\phi_\nu(u)$$

For t=0: $\phi_\nu(u) = e^{i\nu u}$, $\chi = -\frac{(4+\nu^2)}{R^2}$

$u=\ln(z_0/z)$ in ADS corresponds to $\ln(k/k_0)$ in BFKL

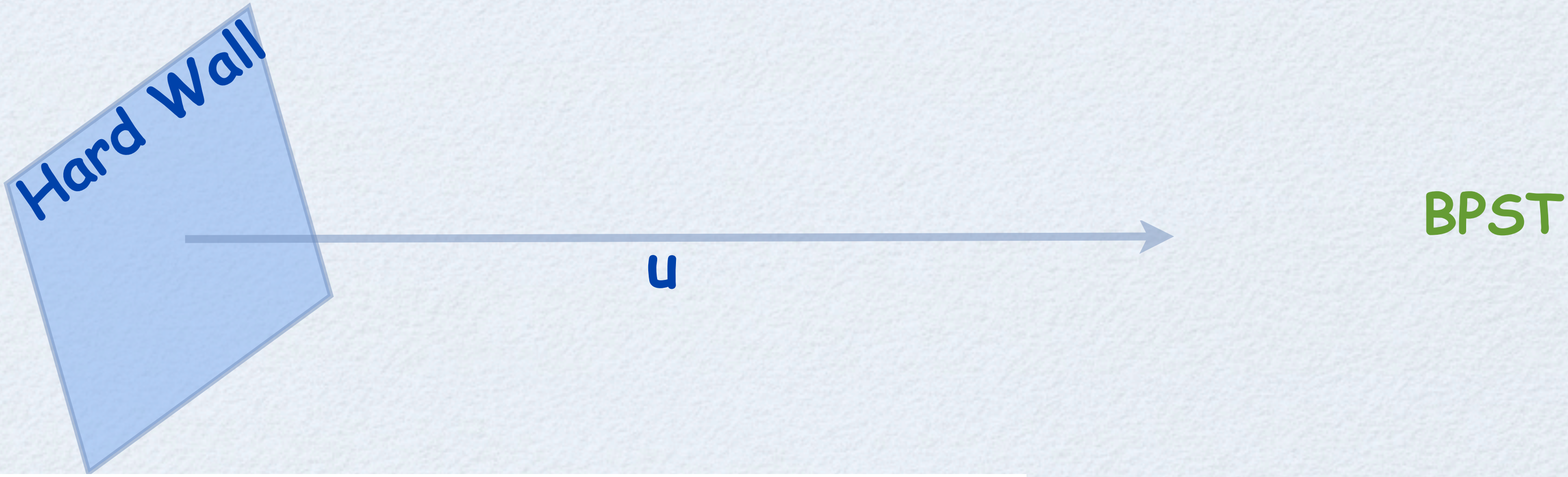

For $t = 0$ eigenfunctions are

$$\phi_\nu(u) = e^{-i\nu u} + R_0(\nu) e^{+i\nu u}$$

eigenfunctions are composed of a plain and a reflected wave

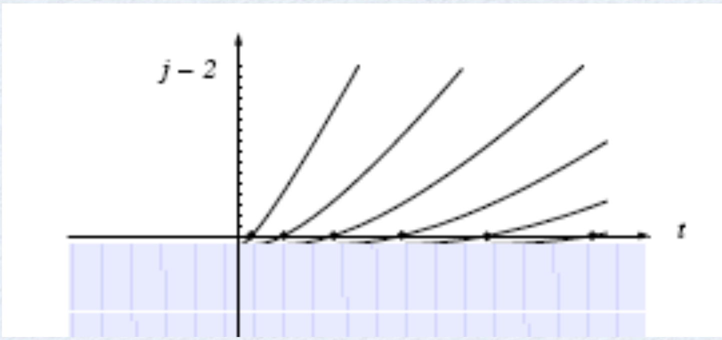

for t>0 the Hard Wall model leads to glueballs, which are the discrete spectrum of 'cavity modes' of the Laplacian for a five-dimensional spin-two field

Pomeron Regge trajectories in ADS

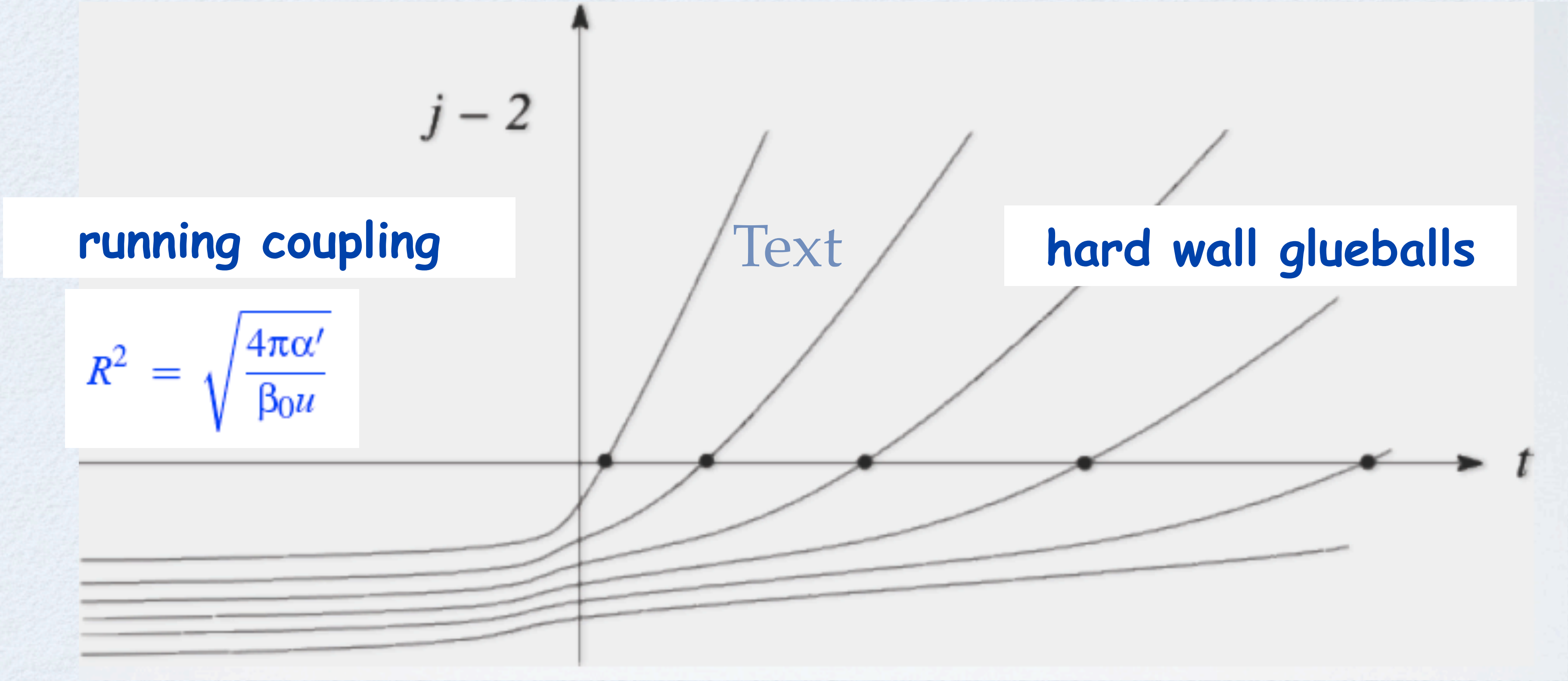

Pomeron and Gauge/String Duality

Brower, Polchinski, Strassler, and Tan, hep-th/0603115

Pomeron is a coherent color-singlet object, build from gluons, with universal properties; it is the object which is exchanged by any pair of hadrons that scatter at high energies.

$$j^0 = 2 - \frac{2}{\pi\sqrt{\bar{\alpha}_s}}$$

in ADS_5 and in N=4 Super YM

Kotikov, Lipatov, Onishchenko, Velizhanin, Physt. Lett. B 632, 754 (2006)

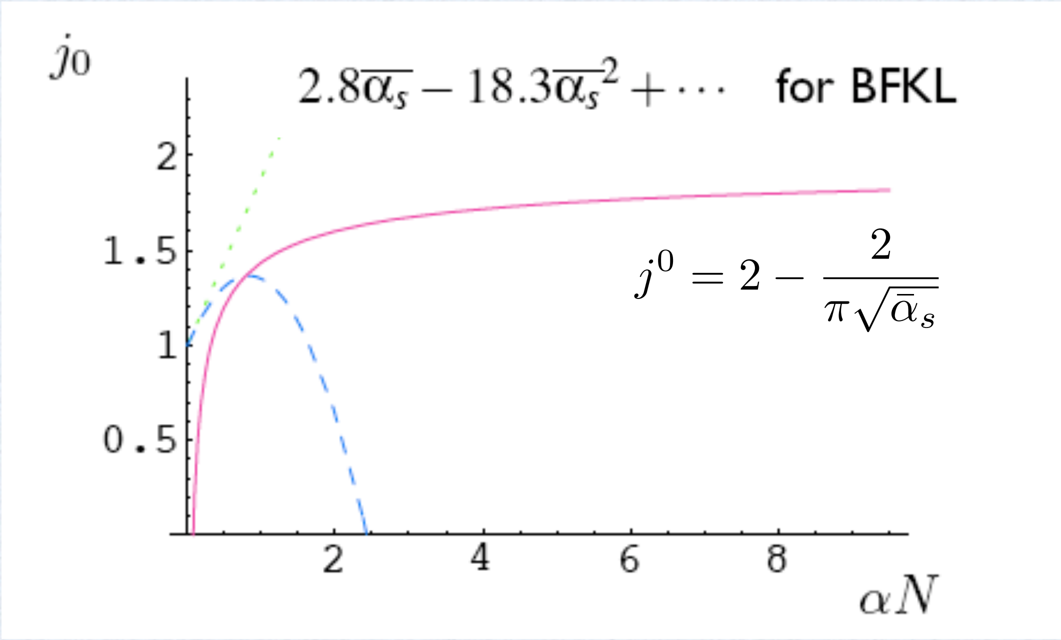

$$\left(\overline{\alpha_s} = \frac{\alpha_s N_C}{\pi}\right)$$

String-Gauge Dual Description of Deep Inelastic Scattering at Small-x

arXiv: 1007.2259v2, Sept 2010

Richard C. Brower,* Marko Djurić,† Ina Sarčević,‡§ and Chung-I Tan¶

diffusion term reflected term

$$F_2(x,Q^2) = \frac{g_0^2 \rho^{3/2}}{32\pi^{5/2}} \int dz dz' P_{13}(z,Q^2) P_{24}(z')(zz'Q^2)\, e^{(1-\rho)\tau} \left(\frac{e^{-\frac{\log^2 z/z'}{\rho\tau}}}{\tau^{1/2}} + \mathcal{F}(z,z',\tau) \frac{e^{-\frac{\log^2 zz'/z_0^2}{\rho\tau}}}{\tau^{1/2}} \right)$$

$P_{13}(z) \approx C\delta(z - 1/Q)$. $\quad P_{24}(z') \approx \delta(z' - 1/Q')$.

$e^{(1-\rho)\tau} \sim (1/x)^{1-\rho}$

$$\mathcal{F}(z,z',\tau) = 1 - 2\sqrt{\rho\pi\tau}\, e^{\eta^2} erfc(\eta), \qquad \eta = \frac{-\log\frac{zz'}{z_0^2} + \rho\tau}{\sqrt{\rho\tau}}.$$

reflected term (model dependent) corresponds to the phase condition in KLRW

fitted variables,
g_0, ρ, z_0, Q'

in KLRW, ρ is predicted

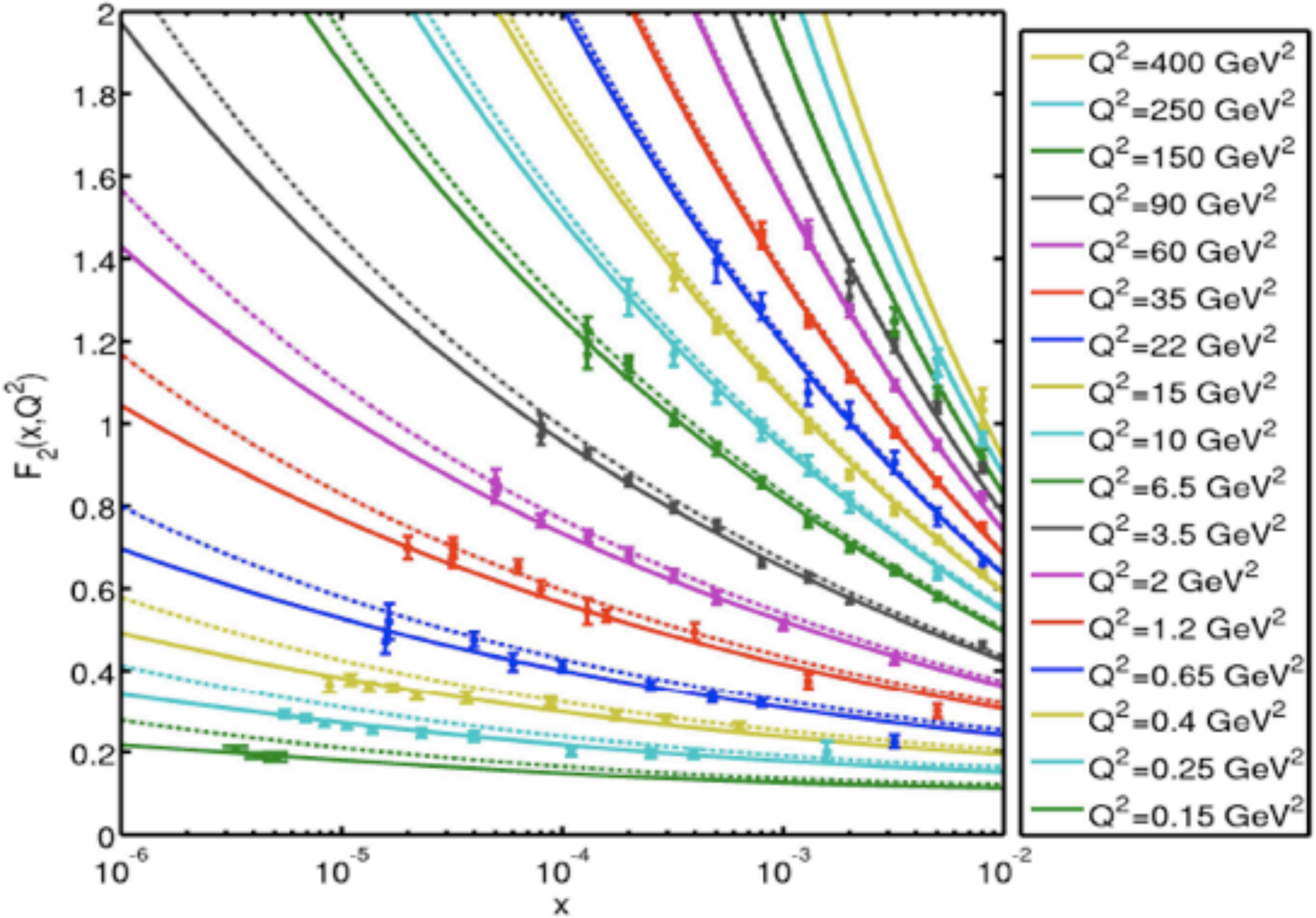

Figure 9: Fit to the combined H1-ZEUS small-x data for $F_2(x,Q^2)$ by a hard-wall eikonal treatment. We have exhibited both the hard-wall single Pomeron fits, (in dashed lines), and the hard-wall eikonal, (in solid lines), together for a better visual comparison. The fit include 249 data points, with $x < 10^{-2}$, and 34 Q^2 values, ranging from 0.1 GeV^2 to 400 GeV^2. Only data set for 17 Q^2 values are shown.

HERA vs LHeC region: dots are H1-ZEUS small-x data points

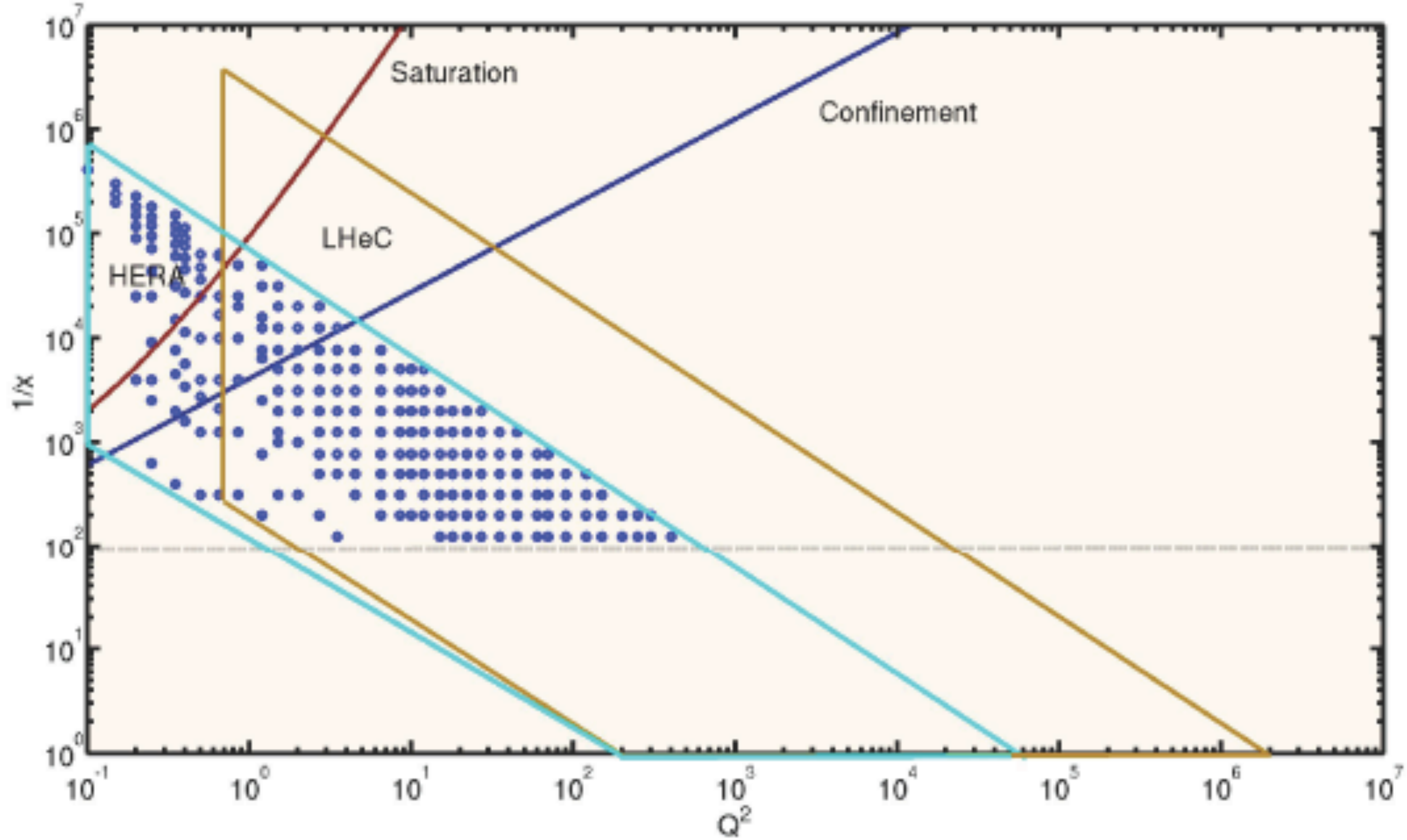

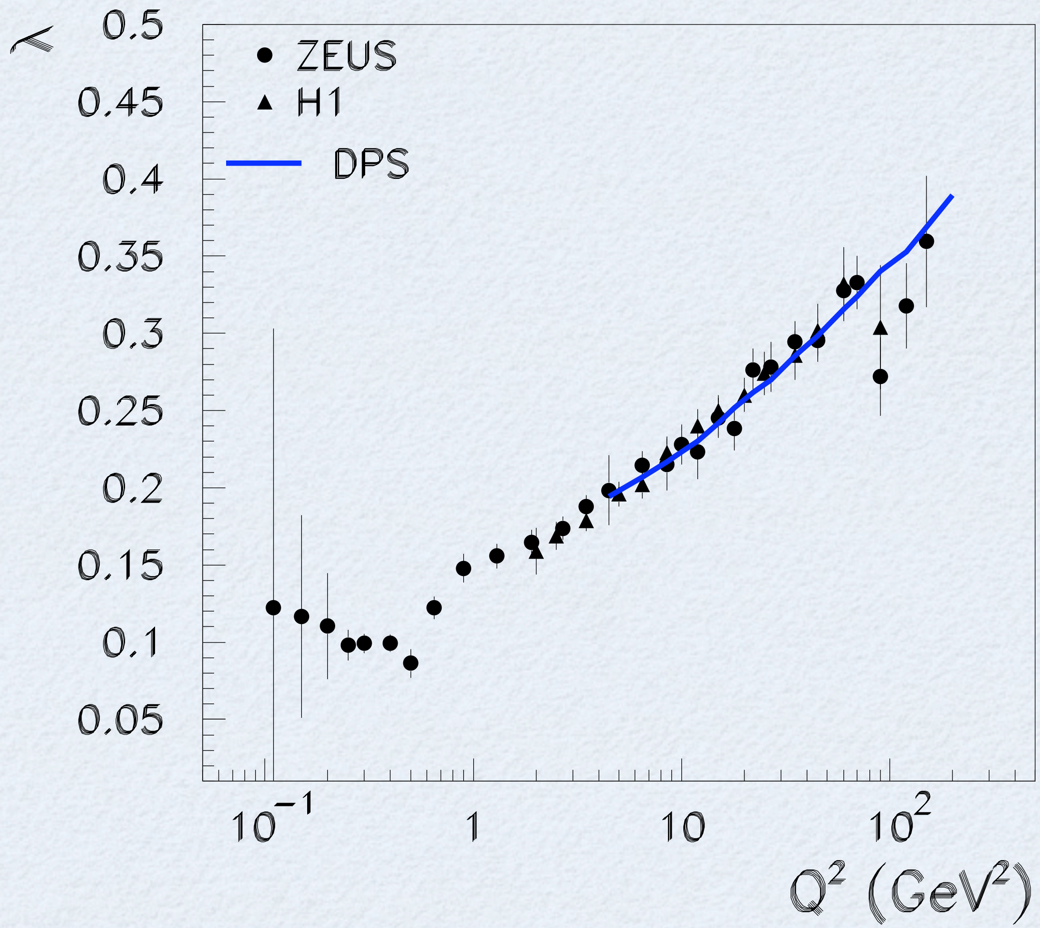

λ
0.5
0.45
0.4
0.35
0.3
0.25
0.2
0.15
0.1
0.05
ZEUS
H1
DPS
10^{-1}
1
10
10^2
Q^2 (GeV^2)

Why to investigate Gluon Density?

- it determines important physics reactions, like Higgs or gluonic di-jet production, at LHC

- Gluon Density ≡ Pomeron determines the high energy behavior of scattering amplitudes

  high energy behavior of scattering amplitudes is connected to the long range behavior of nuclear forces ⇒ confinement

- it is a fundamental physics quantity

Vector Mesons

KMW
PRD 74 074016
PRD 78 014016

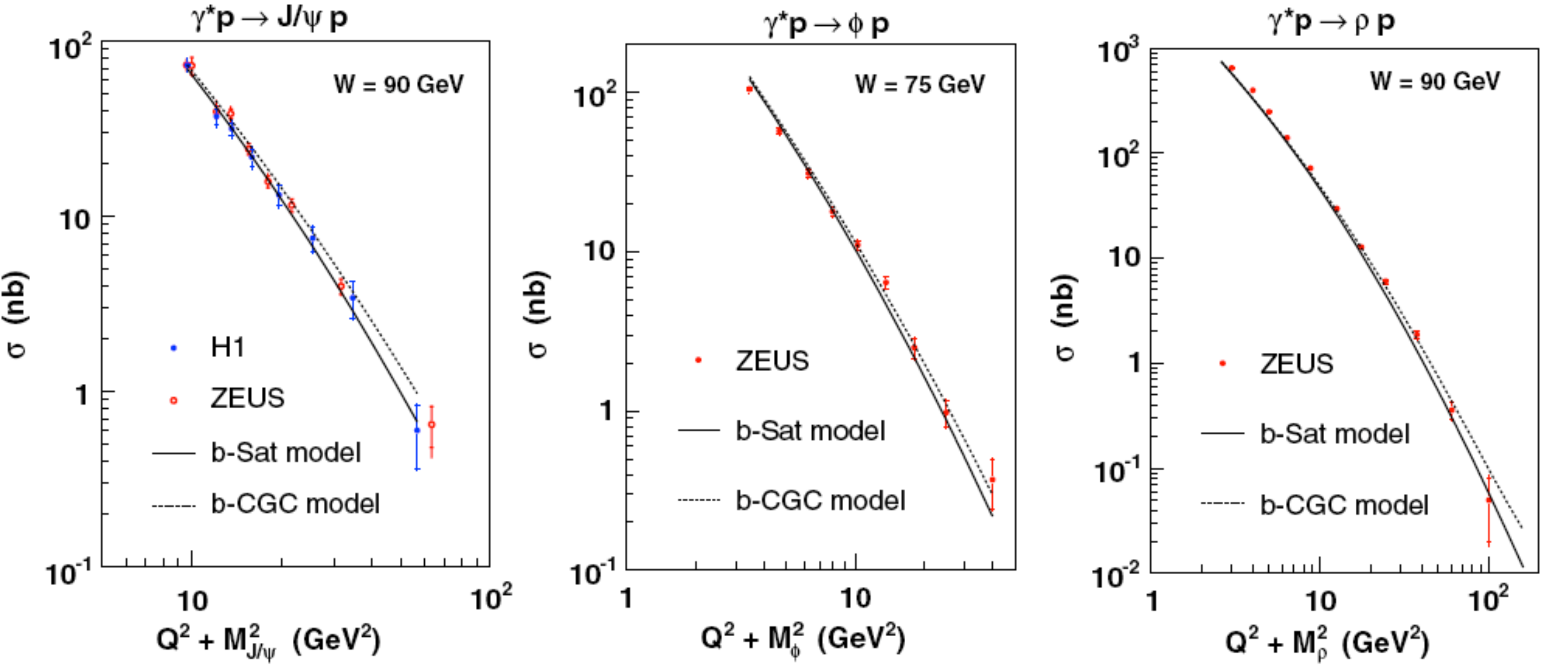

Note: educated guesses for VM wf are working very well